Delft University of Technology
Faculty of Electrical Engineering, Mathematics and Computer Science
Delft Institute of Applied Mathematics

Estimation of the water-gas-ratios of gas wells offshore by a data-driven model

A thesis submitted to the
Delft Institute of Applied Mathematics
in partial fulfillment of the requirements

for the degree

MASTER OF SCIENCE
in
APPLIED MATHEMATICS

by

MARGRIET T.A. NIEUWENHUIS

Delft, The Netherlands
September 2014

MSc thesis APPLIED MATHEMATICS

"Estimation of the water-gas-ratios of gas wells offshore by a data-driven model"

MARGRIET T.A. NIEUWENHUIS

Delft University of Technology

Responsible professor and daily supervisor	**Daily supervisor(NAM)**
Prof.dr.ir. A.W. Heemink	Dr.ir. M. Hooimeijer

Other committee members

Dr.ir. M.B. van Gijzen	Dr.ir. W.T. van Horssen

September, 2014 Delft

Abstract

The Nederlandse Aardolie Maatschappij (NAM) operates about 90 (small) gas fields offshore. During the process of producing gas, water is also produced. The water production originates from the aquifer, below the gas reservoir that contains water, and condense water, dissolved in the gas. The amount of produced water gives valuable information about several aspects of the gas production process; for example the amount of gas left in the well. Therefore, the water production per well is required. However, there are no facilities to measure the water rate for individual wells.

The goal of this research is to investigate if it is possible with the gas data per well and the water production data for several wells together, to construct a model that makes precise yet realistic estimates of the water production. The water production is indicated by the water-gas-ratio (WGR) and the current estimates of these ratios are fluctuating too much. Precise estimates of the WGR means that the model keeps the difference between the estimated and produced water production as small as possible. Realistic estimates of the WGR are defined as (1) the WGR does not decrease over the year and as (2) the WGRs of the different wells are of the size as expected by the production programmer, who gains information from well tests.
The allocation problem can be written as a minimization problem where the objective function is defined as the difference between the measured and estimated water production and constraints are added to ensure the requirements of realistic WGRs. It is solved by applying a least-squares method (LSM). The WGR is assumed constant for a longer period to limit the amount of variables (instead of estimating a WGR every day for every well).

First a model for a small-scale area is constructed. This model shows good results: the estimates of the WGR look similar to the current estimates but do not fluctuate that much. They show only increasing behaviour, which is more realistic. A relative error of 5% is made, which is small.
After that the model is applied to a large-scale area. The area contains more gas fields and wells, making it harder to notice trends for the WGR and see what realistic behaviour for the ratios is. The model results in realistic estimates of the WGR, however, the relative error is $\approx 25\%$.
This model was used to construct the final model: the model of the large-scale area with the errors of the measurements incorporated, which were neglected until now, by applying weighted LSM. The model is run 50 times with the measurements drawn from a Gaussian distribution. The results are used to construct 95%-confidence intervals of the WGRs. The intervals and the error made are large, which means that the estimates are not precise. Overall it is concluded that it is very hard to construct a model based on gas and water production data, that can make precise and realistic estimates of the WGR.

Three suggestions are made to improve the model. The first recommendation is to apply weighted LSM to deal with the fluctuating behaviour of the data. Secondly, the use of the well test could be extended, since these measurements are very accurate. One way to do this, is suggested in the last recommendation; by changing from a data-driven model to a full dynamic model. This means that more physical aspects of the production process are taken into account. The model could be updated or validated by the information from the well tests.

Acknowledgements

After a little more than seven years my study is done and although time flew, I have enjoyed every minute of it. This report contains the results of my master thesis. This is the final step in the study to obtain my masters degree in Applied Mathematics at the Delft University of Technology and was carried out for the Nederlandse Aardolie Maatschappij in Assen.

I would like to thank some people for their support and help during these past nine months. First of all I would like to thank Professor Arnold Heemink for guiding me during the project and bringing me back on track when I was lost. Furthermore I would like to thank Martijn Hooimeijer for giving me the opportunity to do my thesis at the Nederlandse Aardolie Maatschappij and always asking critical questions which helped me to understand what was going on. Also I would like to thank Ivo Heitman for explaining me the details of offshore gas production and much more during my visits to Assen. I would like to thank Liselot Arkesteijn for reading my report and providing me with useful comments on it.

Most importantly I would like to thank my parents for giving me the opportunity and always supported me to develop myself during my study. Last but not least, I would like to thank my family and friends for all relaxing times we had at university, on court, at the bar or any other place which helped me to de-stress and not to think of all the work I had to do.

Margriet Nieuwenhuis
September 30, 2014

Contents

Glossary

Acronym	**Meaning**
bbl	Barrel, has a content of 119 L
bbl/MMscf	The amount of barrels water produced per MMscf of produced natural gas
LSM	Least squares method
MMscf	Million cubic meters per square feet, common unit for oil and gas
NAM	Nederlandse Aardolie Maatschappij
Platform PB	Platform Barque PB, satellite platform of Clipper
Platform PG	Platform Galleon PG, satellite platform of Clipper
Platform PL	Platform Barque PL, satellite platform of Clipper
Platform PN	Platform Galleon PN, satellite platform of Clipper
Platform PS	Platform Skiff PS, satellite platform of Clipper
Platform PW	Platform Clipper PW, satellite platform of Clipper
WGR	Water-gas-ratio, the amount of water in m^3 produced per m^3 produced gas
WLSM	Weighted LSM, where the weight indicates per equation the contribution of that equation to the objective function

Symbols

Symbol	**Meaning**
Δ	maximum fraction between WGR of different wells on the same day/period
G	gas production data of N wells on n days
n	number of days data is available
N	number of wells in an area
N_{nw}	number of wells in an area with a WGR of no significant size
N_w	number of wells in an area with a WGR of significant size
Q	number of periods the WGR is estimated, equal to n/T
r	WGR of N wells on n days/Q periods
σ_w	standard deviation of the measurement error of the water production
σ_g	standard deviation of the measurement error of the gas production
T	days WGR is assumed constant for
w	water production data on n days, given as the sum over N wells
W	weight used during the WLSM

Chapter 1

Introduction to the problem

This chapter first gives an introduction to the Nederlandse Aardolie Maatschappij (NAM). Next the details of the gas production offshore are given. After that an explanation of the current situation is formulated.

1.1 Introduction to the NAM

In 1943 the Shell company Exploratie Holland finds oil in the Dutch soil. Shortly after the second World War, Shell and Esso decide to establish a company to invest together in the search for oil. This resulted in the establishment of the Nederlandse Aardolie Maatschappij(NAM) in 1947. After the discovery of the large gas field in Slochteren, NAM decides to focus on the search for natural gas instead of oil (NAM, 2014). Ever since, NAM has been looking for new gas fields, both on- and offshore. The offshore drilling for natural gas started in 1961 in the North Sea. Now NAM operates about 90 (small) gas fields at the North Sea, which are produced from several hundred wells, across 50 offshore platforms. The offshore gas network at the North Sea is shown in Appendix A.

1.2 Introduction to gas production offshore

Below an introduction to gas production in general and to gas production offshore is given.

1.2.1 Gas reservoir

Figure 1.1 shows a cross section of the layers in the gas reservoir.

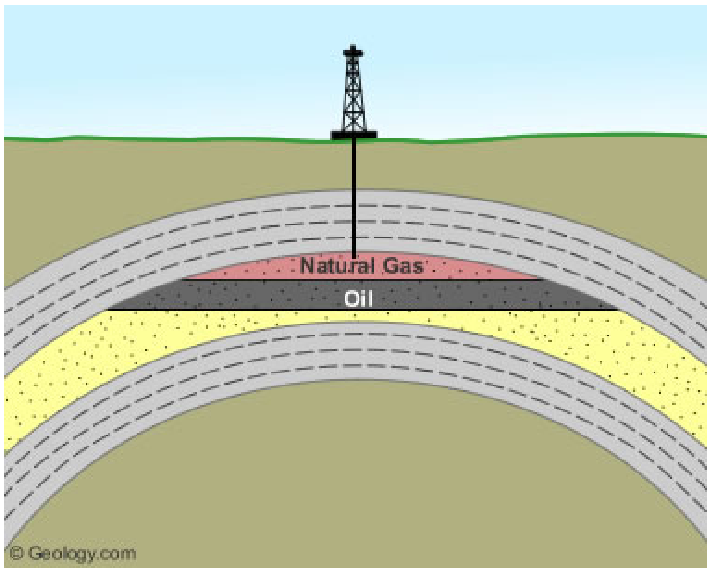

FIGURE 1.1. Cross section gas reservoir (Geology.com, 2014)

Notice that this is a cross section onshore, however, offshore reservoirs are similar (the upper green layer is water). The gray layer can be clay or hard stone and the yellow dotted layer is water, which is called the aquifer. Note that the oil and gas layer are not that strictly separated as illustrated here. The separation of the layers can for example be as illustrated in Figure 1.2.

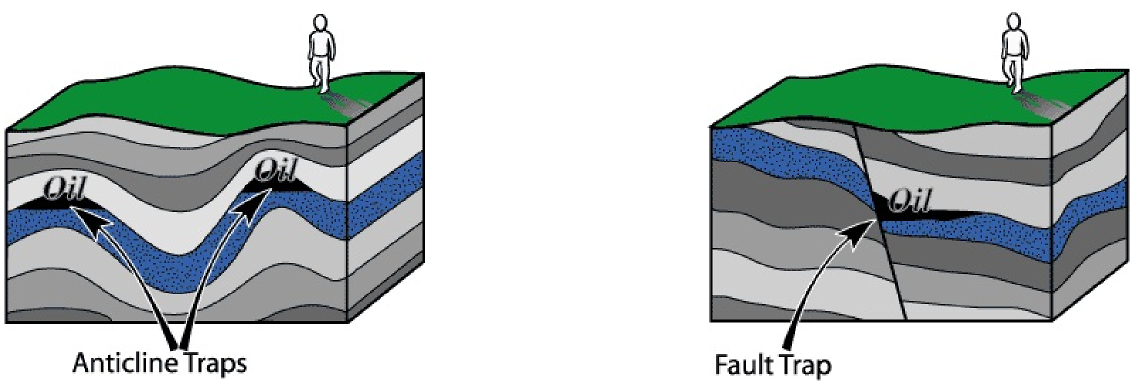

FIGURE 1.2. Different designs of cross section gas reservoir (The Paleontological Research Institution, 2014)

Again for the gray layers one can think of stone. Although this figure contains oil reservoirs, the same principles apply to gas. From the figure one can see that every reservoir has its own size, contour and surroundings, such that every well produces different amounts of gas and water. The production behaviour develops differently for all wells throughout the lifetime of a well.

As natural gas is produced, the pressure in the gas layer drops. This causes the layers below the gas layer to rise up. This means that the composition of the produced mixture changes over the time; the water/gas fraction will increase. When the water production increases too much, one speaks of water break-through; it is less profitable to operate the well and it is shut down.

1.2.2 Details of gas production offshore

Producing gas offshore requires other preparations compared to natural gas produced onshore, because of logistical challenges. The various liquids that are present in offshore produced gas, are described below:

1. Condensate: this liquid consists of small droplets of liquid carbon hydrates that are produced with the gas.
2. Condense water: water that is dissolved in the gas (similar to the water dissolved in air). As the pressure decreases when the gas is pumped up, the water condenses.
3. Formation water: water from the aquifer below the gas layer, which is more saline than sea water. As explained above, this amount can increase over time as gas is produced.

The size of the condensate production can be neglected and hence the last two liquids are considered as the total water production of a well. The amount of produced water, gives information about and influences several aspects of the gas production process:

- The connection of the well to the gas layer. The length of the pipeline that is in the gas layer, influences the amount of produced gas. In this well perforations are made such that the gas can flow into the well. If the perforations are made close to the aquifer, the chance of producing formation water, increases.
- The amount of gas left in the well. The formation water layer can come up if the amount of gas in the gas layer decreases. More water in the fluid might indicate that the formation layer has come up to the well which indicates that the well has been producing gas for some time.
- The amount of MEG (Mono-ethylene glycol) that has to be added to the fluid. MEG is a kind of antifreeze and hence prevents the fluid from freezing when it is pumped up. Since the estimates of the water production are not very accurate right now, the amount of MEG is chosen with a safe margin. However, this MEG also has to be removed from the fluid when it reaches the shore. Thus the amount of MEG that is added can be lowered which results in less work and time when the gas is prepared for usage.

1.3 Problems with the water-gas-ratio estimation

Data is available on the gas production per well and on the water production as the sum over a number of (depending on the platform) wells together. However, the water originates from the wells and the amount is dependent on the water-gas-ratio (WGR). This fraction indicates the amount of water produced per unit of produced gas. Although the water production is measured as the sum over several wells, knowing the water production per well gives valuable information as stated above. However, NAM currently has not yet developed a precise method to allocate the total water production to the wells producing it (as there are no facilities to measure the water rate for individual wells).

1.3.1 The available data

To gain insight in the behaviour of the WGR, Figure 1.3 shows the gas and water production of platform Sean PD in 2012. This platform will be used in the development of the complete algorithm for a more complicated area, Solepit. Notice that the amount of gas is summed over all wells. Both volumes are given in standard cubic meters (Sm^3), which is equal to the amount of gas that has the volume of one cubic meter at zero degrees Celsius at atmospheric pressure (1.013 bar).

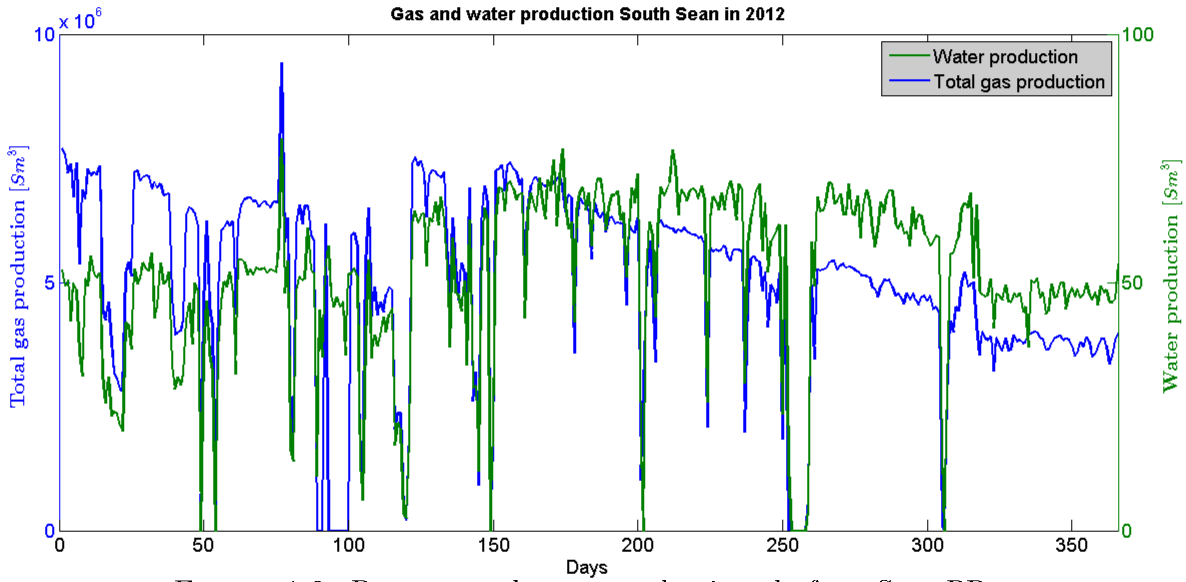

FIGURE 1.3. Data gas and water production platform Sean PD

In the early life of the field, the Sean field was used as a wing producer (instead of producing at a constant level, the field was used to complete the total demand). Since March 2012 a blow down strategy is applied to the field (Heitman, 2014a). This means that the wells are producing on their maximum capacity. As a result this maximum capacity is decreasing, which results in a downwards trend of gas production. This explains the behaviour in Figure 1.3; in the first part of the year the gas production is fluctuating a lot but after that it is more stable. The water production on the other hand, is of roughly the same size over the year. Thus when we are looking for the WGRs, it can be kept in mind that an increasing trend is expected.

1.3.2 Current allocation algorithm

The current algorithm for the water allocation process is based on the gas volume produced and an assumed WGR (which may vary per well and over time). An example of a WGR as it develops over time, is provided in Figure 1.4.

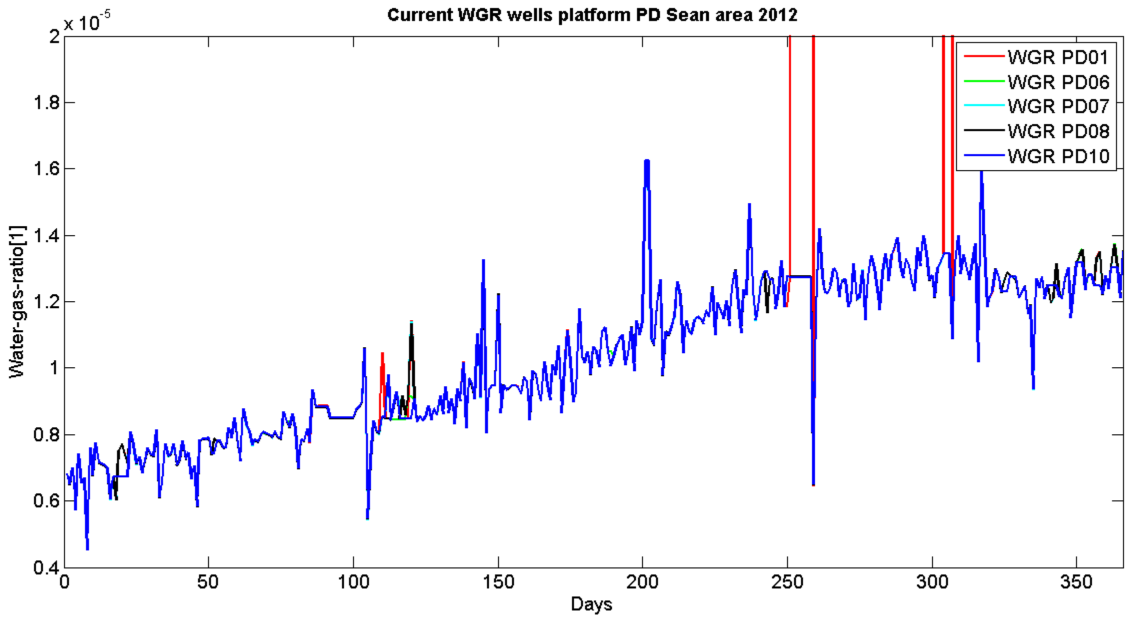

FIGURE 1.4. Current WGR estimates PD platform Sean area, 2012

From Figure 1.4 it can be concluded that the WGRs of all wells show similar behaviour for this field (the lines which are not visible are below another line). Furthermore, one can see that on some days the WGR of well PD01 is very large, which is most likely to be an error in the measurements or an indicator that perhaps uncertainties or time delays are present in this process. Such big changes are not realistic as significant changes in the WGR can only occur over longer periods than a day. For example a few weeks or a month (Heitman, 2014a). This allocation process, however, shows that the estimated behaviour is unrealistic, it changes too much and too fast to give a realistic pattern.

1.3.3 Problem statement

The goal of this research is to investigate whether it is possible with the available gas and water data to construct a model to make more precise, yet realistic estimates of the water production per well. Precise estimates means that the error (difference between the measured and estimated production water) is as small as possible. An estimated WGR is defined as realistic if (1) WGRs which can only increase (exceptions allowed under specific circumstances) and (2) the size of WGRs is of the expected order based on the knowledge of the production programmer.

The problem can be approached by answering sub-questions, which will contribute to the development of the model that meets the above criteria:

1. How can the problem be described mathematically?
2. What is the best solution method to solve the problem?
3. How can the solution method be implemented to solve the problem for a small-scale area?
4. What extensions are needed to solve the problem for a large-scale area and how can this be implemented?

1.4 Outline of the report

The first two sub-questions are answered in the second chapter. The implementation and the results of the small-scale area are presented in chapter 3. The extensions and results for the larger area are given in chapter 4. This chapter also contains the complete model where all aspects of the area, including the uncertainties, are implemented. After these steps a chapter follows with the concluding remarks and recommendations for further research.

Chapter 2

Formulation and background of the minimization problem

This chapter explains the problem in more detail. First the mathematical formulation of the problem is given, which results in a minimization problem. After that, the solution method is discussed and applied to the problem. At the end of this chapter the algorithm to solve this type of minimization problems is explained.

2.1 General mathematical formulation

The production of the gas is given per well, while the production of water on the other hand is given as the sum over all wells together. Each well has a WGR which depends on several properties of the well, for example how much gas is left in the well. The goal is to find a realistic WGR for all wells (on every day), such that the error between the estimated and produced water is as small as possible. Define $\varepsilon = (\ldots, \varepsilon_j, \ldots)^T$, the $n \times 1$ vector containing the errors on every day and $r = (\ldots, r_j^T, \ldots)^T$ the $(n * N) \times 1$ vector containing the WGRs on every day.

$$\min_r \quad ||\varepsilon(r)||_p \qquad \text{with } \varepsilon_j = w_j - G_j r_j \tag{1}$$

$$s.t. \quad r_j \geq 0 \qquad j \in \{1, \ldots, n\} \tag{2}$$

ε	is a $n \times 1$ vector of errors made on the days
r_j	is a $N \times 1$ vector of WGRs to be estimated. They are ratios, hence positive.
w_j	is the measured water production on day j.
G_j	is a $1 \times N$ matrix of the measured gas production on day j

for some integer (or ∞) p whose size depends on how the difference between the estimated and produced water should be considered. For example, for $p = 1$ the sum of the absolute values is minimized and when $p = \infty$ the supremum of the differences is minimized. In this minimization problem the dependent variable is w_j, the independent variable is G_j and r_j is the regression coefficient.

2.1.1 Adding constraints

From the above minimization problem it is not immediately clear that realistic WGRs are estimated. In the first chapter 'realistic' is defined in two parts. The first requirement is that the WGR can only increase, since it is a physical property of the well which can not suddenly decrease. The following constraint is introduced:

$$r_j \geq r_{j-1} \quad j \in \{2, \ldots, n\} \quad \text{which should hold elementwise}$$

The second requirement is that the size of the WGRs are of the order as expected by the production programmer, who gains information from well tests. These are very accurate tests which measure for example the WGR, but they are expensive and thus not executed often. On average the test is performed once a year, but this differs per platform (a well with abnormal behaviour is investigated more frequently compared to platforms where this is not the case). A constraint can be added to relate the size of the WGRs for different wells to each other by a certain factor. This constraint is formulated and the size of this factor is chosen for each of the areas considered in this report seperately, depending on the information from the well test.

2.1.2 Adaption problem

The minimization problem has to be solved for every day. Each day one equation is available, whereas the amount of estimated ratios is equal to N (the number of wells in the area). This means that the system is underdetermined and has infinitely many solutions. Therefore the WGR is assumed constant for a certain period.

Suppose that the WGR is assumed constant for a period of T days resulting in $Q = n/T$ periods. Define $\widetilde{\varepsilon} = (\ldots, \widetilde{\varepsilon}_i, \ldots)^T$, still a $n \times 1$ vector, and $\widetilde{r} = (\ldots, \widetilde{r}_i^T, \ldots)^T$, a $(Q * N) \times 1$ vector. The minimization problem changes to:

$$\min_{\widetilde{r}} \quad ||\widetilde{\varepsilon}(\widetilde{r})||_p \qquad \text{with } \widetilde{\varepsilon}_i = \widetilde{w}_i - \widetilde{G}_i \widetilde{r}_i \tag{3}$$

$$s.t. \quad \widetilde{r}_i \geq \widetilde{r}_{i-1} \qquad i \in \{2, \ldots, Q\} \tag{4}$$

$$\widetilde{r}_i \geq 0 \qquad i \in \{1, \ldots, Q\} \tag{5}$$

$\widetilde{\varepsilon}$	is a $n \times 1$ vector of errors made at the days. Each $\widetilde{\varepsilon}_i$ is a $T \times 1$ vector.
$\widetilde{r}_i$	is a $N \times 1$ vector of WGRs to be estimated.
$\widetilde{w}_i$	short for $w_{i:i+T}$ which is a $T \times 1$ vector of the measured water production on day $i : i + T$.
$\widetilde{G}_i$	short for $G_{i:i+T}$ which is a $T \times N$ matrix of the measured gas production on day $i : i + T$.

The period over which the estimate of the WGR is assumed constant, is not exactly known. For the current problem, every period Q there are T equations available and N variables to be estimated. Thus, for this problem to be overdetermined it should hold that $T > N$ where $n = TQ$.

2.2 Least-squares method

The most applied regression model to solve regression problems is the least-squares method (LSM). This means that in the minimization problem (3)-(5), $p = 2$ is chosen:

$$\min_{\widetilde{r}} \quad ||\widetilde{\varepsilon}(\widetilde{r})||_2 = \sqrt{\sum_{i=1}^{Q} \left(\widetilde{w}_i - \widetilde{G}_i \widetilde{r}_i\right)^2} \tag{6}$$

where $\widetilde{\varepsilon}$ and $\widetilde{r}$ are defined as in (3)-(5). Aspects of the LSM are listed below:

- The LSM is easy to implement and is very fast.
- The LSM is not very robust to outliers. Because the difference between the estimated and measured water production is squared, outliers result in a larger error.
- The problem has to be overdetermined. This means that there need to be at least as many equations as there are variables to be estimated. If there are less equations than there are unknowns, there are degrees of freedom which implies infinitely many solutions. Adding more constraints would reduce the degrees of freedom and might result in a unique solution, however local minima are usually found.
- A minimum always exists: the objective function is a real-valued, convex and differentiable function.

The ordinary LSM can be applied in two ways to the problem. The first one finds the WGRs of the periods in succeeding order, where the result of the previous period is a lower bound for the period following after it. Disadvantage of this algorithm is that it might occur that the WGR of an earlier period is estimated such that the WGR of the period after needs to be estimated too large because of the lower bound (which is based on the previous period). This is why in the second algorithm the problem is solved for the whole year at once. Then it is possible that the WGRs in an earlier period are kept smaller such that the WGRs in a later period fit better.

Suppose that the WGR is kept constant for a period of T days, resulting in a total of Q periods which is equal to n/T. Then the minimization problem is given by:

$$\min_{\widetilde{r}} \quad ||\widetilde{\varepsilon}(\widetilde{r})||_2 \tag{7}$$

$$s.t. \quad \widetilde{r}_i \geq \widetilde{r}_{i-1} \qquad i \in \{2, \ldots, Q\} \tag{8}$$

$$\widetilde{r}_i \geq 0 \qquad i \in \{1, \ldots, Q\} \tag{9}$$

where $\widetilde{\varepsilon}(\widetilde{r})$ is given by:

$$\widetilde{\varepsilon}(\widetilde{r}) = \begin{bmatrix} w_{1:T} - G_{1:T}\ \widetilde{r}_{1:N} \\ w_{T+1:2T} - G_{T+1:2T}\ \widetilde{r}_{N+1:2N} \\ \vdots \\ w_{(Q-1)T+1:QT} - G_{(Q-1)T+1:QT}\ \widetilde{r}_{(Q-1)N+1:QN} \end{bmatrix}$$

2.2.1 Performance of the LSM

To measure the performance of the LSM, the final value of the objective function is considered. This indicates how much the estimated water deviates from the measured water production. The relative error is also important in this estimation process, because it takes the total water production into account while measuring the error. Both error measures are used, because through the value of the criterion of the minimization problem insight is gained in the quality of the estimation model. The relative error on the other hand, tells us more about the error in perspective to the total water production. The relative error is given below:

$$\text{relative error} = \frac{\sum_{i=1}^{Q} |\widetilde{G}_i \ \widetilde{r}_i - \widetilde{w}_i|}{\sum_{i=1}^{Q} \widetilde{w}_i} \tag{10}$$

2.2.2 Uncertainty in the measurements

The measurement errors are given by the NAM as a percentage deviated from the measured value. This means that the measurement errors are Gaussian with the following parameters:

$$w_j + \alpha_j \quad \alpha_j \sim \quad N(0, \sigma_w^2 w_j) = N(0, \sigma_{w_j}^2) \qquad j \in \{1, \dots, n\} \tag{11}$$

$$G_j^k + \beta_j^k \quad \beta_j^k \sim \quad N(0, \sigma_g^2 G_j^k) = N(0, \sigma_{g_j^k}^2), \qquad j \in \{1, \dots, n\} \quad k \in \{1, \dots, N\} \tag{12}$$

The errors from day to day are assumed to be uncorrelated:

$$E(\alpha_j \alpha_i) = 0 \qquad \forall j \neq i \tag{13}$$

$$E(\beta_j \beta_i) = 0 \qquad \forall j \neq i \tag{14}$$

Problems where the dependent variable is uncertain, are adapted to weighted least squares. This means that some of the equations get a higher weight (=are taken more into account), namely those equations of which the data is more certain (Nocedal and Wright, 2006). The weight is equal to 1 divided by the variance of the measurement; each row of the $\widetilde{\varepsilon}$ in the minimization problem is multiplied by the vector W_i, where $i \in \{1, \dots, Q\}$, containing the weight per day. The weights of the first period are given by the vector W_1:

$$W_1 = \begin{bmatrix} W_1^1 \\ W_1^2 \\ \vdots \\ W_1^T \end{bmatrix} = \begin{bmatrix} \frac{1}{\sigma_{w_1}^2} \\ \frac{1}{\sigma_{w_2}^2} \\ \vdots \\ \frac{1}{\sigma_{w_T}^2} \end{bmatrix}$$

The uncertainty in the independent variable is investigated by solving the model several times each with differently perturbed gas numbers. The mean and standard deviation of the solution sets will be determined. With these numbers the 95%-confidence interval of the WGRs is constructed, to gain insight in how precise the estimates are. A large interval indicates that the estimates are not precise.

2.3 Algorithm

Below information is given about algorithms to solve constrained minimization problems. For convenience a general minimization problem is used here. Suppose the minimization problem is given by:

$$\min_{x} \quad f(x) \tag{15}$$
$$s.t. \quad c_i(x) = 0 \qquad i \in \mathcal{E} \tag{16}$$
$$c_i(x) \leq 0 \qquad i \in \mathcal{I} \tag{17}$$

where $\mathcal{E}, \mathcal{I}$ are two finite sets of indices and the functions c_i are smooth.

When there are only equality constraints present, the method to handle the constraints is by Lagrange-Multipliers:

$$\min_{x,\lambda} \widetilde{f}(x,\lambda) = f(x) - \lambda \sum_{i \in \mathcal{E}} c_i(x) \tag{18}$$

This results in an unconstrained minimization problem for which many algorithms are available (Nocedal and Wright, 2006). There are a lot of solution algorithms, however since the problem in this report is large most of these algorithms, for example Newton methods, are not suitable. These algorithms need higher-order derivatives of the objective function which is computationally expensive. Gradient-based algorithms only need to compute the gradient and are hence able to deal with large problems.

The inequality constraints are more difficult to handle, because it is impossible to formulate the minimization problem as an unconstrained minimization problem, as with equality constraints. There are several algorithms available to solve a inequality constrained minimization problems. The two most applied algorithms in the last few decades (Nocedal and Wright, 2006) are given below with a short description of their strategy:

(1) **Active set** An active set is defined as the points where the constraints show equality. For most minimization problems it is not immediately clear what the active set exactly is and determining this set is the main challenge for inequality-constrained minimization problems(Nocedal and Wright, 2006). There are three types of active-set methods: primal, dual and primal-dual. The primal active-set method is the only method where the iterates are in the feasible region while the objective function is decreased. The algorithm first seeks for the best step size, after which the direction of the step is determined. This is done by solving sub-problems where during the first sub-problem the constraints are temporarily disregarded (Nocedal and Wright, 2006).

(2) **Interior point** The minimization problem is formulated a little bit different with this method:

$$\min_{x,s} \quad f(x) \tag{19}$$
$$s.t. \quad c_i(x) = 0 \qquad i \in \mathcal{E} \tag{20}$$
$$c_i(x) + s = 0 \qquad i \in \mathcal{I} \tag{21}$$
$$s \geq 0 \tag{22}$$

The derivation of interior-point methods associates (19)-(22) with the barrier problem (Nocedal and Wright, 2006):

$$\min_{x,s} \quad f(x) - \mu \sum_{i \in \mathcal{E} \cup \mathcal{I}} \log(s_i) \tag{23}$$
$$s.t. \quad c_i(x) = 0 \qquad i \in \mathcal{E} \tag{24}$$
$$c_i(x) + s = 0 \qquad i \in \mathcal{I} \tag{25}$$

where μ is a positive parameter. Letting μ converge to zero, the sequence of solutions to the above minimization problem should normally converge to a stationary point of the original problem (15)-(17). An initial μ is chosen and then the barrier problem is solved (this can be done by many algorithms, but is out of the scope of this report see (Nocedal and Wright, 2006) for details). Then μ is updated and the process is repeated.

The active-set method is computational expensive for large problems. Therefore the choice for an interior-point method is made. This algorithm is available in MATLAB, the programme used to compute the model. The interior-point algorithm in MATLAB uses a trust-region-method to solve the barrier problem. Furthermore, finite-differences are used to compute the gradient during the optimization process.

Chapter 3

Small-scale model

This chapter explains how the model is applied to a small-scale area. First some notes regarding the implementation are given. After that the results for the small-scale problem will be presented and some first conclusions are drawn.

3.1 Implementation algorithm on simplified small-scale platform

A schematic overview of the area under consideration for the small-scale problem is shown in Figure 3.1.

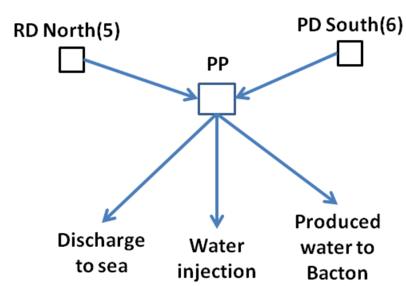

Figure 3.1. Gas and water flows at the Sean area

The number in between brackets indicates the number of wells at the satellite platforms RD North and PD South. The water is collected at the PP platform from where there are three options possible to deal with the water. In 2012, almost all water was injected into the wells and no water was discharged to the sea. However, there might always be circumstances under which this changes. The fluid that is transported to Bacton contains the condensate (oil or other carbon hydrates) where it will be prepared for production.

In Appendix A a map of the above area can be found with details about distances and cross sections of the pipelines. For the Sean area the distances are small (a few kilometers). Hence, the assumption is made that there is no time delay. Furthermore, the assumption is made that the measurements are accurate (no uncertainty taken into account). The data contains some errors or indicates that there is a delay present because there are days that the gas production is equal to zero, while there is a water production.

From the data it was noticed that the gas production numbers are of the order $10^5 - 10^6$ while the water production numbers are of the order 10^1. Thus the WGRs that are being estimated are of the order $10^{-6} - 10^{-5}$. This means that the WGRs are very sensitive; a small change in the WGRs results in a large change in the water production.

3.1.1 Implementation

For the construction of a small-scale model the PD South satellite platform of the Sean area is used. Some adaptions have to be made to the data such that the least-squares method is applicable:

- The number of days: the year 2012 had 366 days. However, since the WGR is assumed constant for a certain period, 366 (or a smaller number close to this) should be dividable by these periods. Hence, we are looking for a set of numbers such that a number close to 366 by which every member of this set is dividable. We picked the total number of days equal to 364 and the set of days the WGR is kept constant for $[7, 13, 28, 52, 91, 364]$ days. Notice that a few of these periods correspond to keeping the WGR constant for a week, roughly two weeks and roughly a month which are good options to investigate. In the previous chapter it was already mentioned that for overdetermination $T > N$ is needed, which holds for all selected periods T.
- Cleaning the data: the data contains some unrealistic occurrences. On some days there is a water production, but no gas production, which is not possible. This is most probably due to measuring errors. Regardless the cause, it increases the error. Thus the water production on these days will be set equal to zero.
- Sweep: an exemption to the constraint in the minimization problem can be made if there was a shutdown in the gas production. How this principle exactly works is explained in section 4.4.1 when a model is constructed for the Solepit area. At the Sean area the amount of long (a couple of days) shutdowns is very small and thus this effect is neglected here.

3.1.2 Additional constraint

As explained in the problem statement, the fraction between the WGRs for different wells should be in line with the knowledge of the production programmer. For the Sean platform it is known that the WGRs of all wells are of the same size, partly caused from the fact that the wells are connected to the same gas field (Heitman, 2014a). Therefore, constraints are added saying that the WGR can not differ more than a factor Δ from the WGR of other wells on the same day:

$$-\frac{1}{\Delta} r_j^{k+1} \quad \leq \quad r_j^k \quad \leq \quad \Delta r_j^{k+1} \qquad j \in \{1, \dots, n\}, \quad k \in \{1, \dots, N-1\}$$

Since the WGRs are assumed to remain constant for a period of T days, the constraint is rewritten into:

$$-\frac{1}{\Delta} \widetilde{r}^{k+1}_{(i-1)N+1:iN} \leq \widetilde{r}^{k}_{(i-1)N+1:iN} \leq \Delta \widetilde{r}^{k+1}_{(i-1)N+1:iN} \qquad i \in \{1, \dots, Q\}, \quad k \in \{1, \dots, N-1\}$$

The value of Δ is assumed to be equal to 2.5, such that the WGRs of different wells are of the same order.

3.2 Results

Now that the minimization problem is completely defined, the WGRs can be solved. Figure 3.2 contains the results of the algorithm for the well PD08, located in the Sean area.

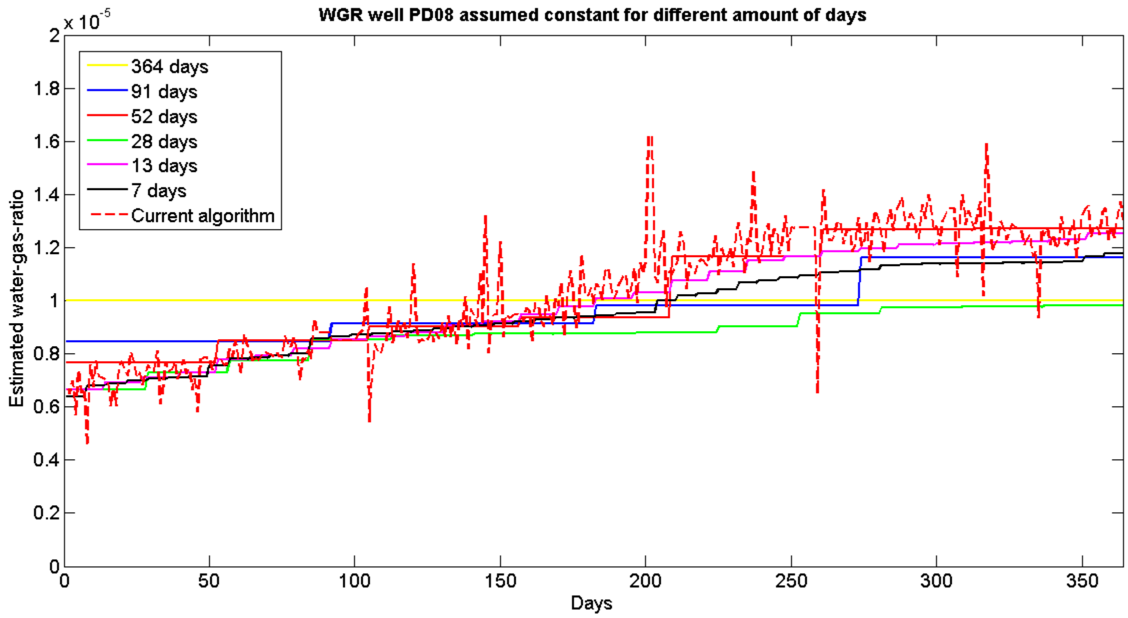

FIGURE 3.2. WGR assumed constant over different periods, well PD08

As can be seen from the figure, the behaviour of the WGR is more fluent compared to the current algorithm. When the period is equal to two weeks or one week, the algorithm produces an increasing estimate of the WGR which is close to the current algorithm. The algorithm produces realistic estimates of the WGR. Note that the estimates of the different periods, perform differently; some of the periods follow the current estimate, where other periods do not. Appendix B contains the estimates for the other wells. Looking at the estimates of all wells, it can be concluded that the size of the estimated WGRs are of the same order, as was required by the production programmer.

An important note here, is that the result of the model is very dependent on the initial guess of the WGR. Different behaviour for the estimates (mainly for $T = 13$ or 7) was observed. The solution shown here was chosen, because it obviously fits the current estimate well. The other behaviours for the WGR that were seen, would especially in the end deviate from the current estimate. The problem has a large solution set consisting of local solutions. The initial guess determines towards which local solution the algorithm converges. During the simulations it was seen that the errors were of similar size for a lot of these local solutions.

3.2.1 Error analysis

In Table 3.1 the error that is being made during the computation, can be found.

WGR constant for	2-norm error	Relative error
364 days	202.8206	18.08%
91 days	88.2604	6.46%
52 days	77.1153	5.69%
28 days	71.4001	4.96%
13 days	71.0615	4.92%
7 days	69.4988	4.76%

TABLE 3.1. 2-norm and relative error Sean algorithm

The errors are small, which means that the algorithm performs well on estimating the measured water production precisely. A relative error of 5% is acceptable and might be caused by some small delays or measuring errors. Note that the error is more or less the same for three different periods. Apparently decreasing the constant period of the WGR from some point on, does not result in a better estimate of the amount of produced water. For the periods of two weeks and one week, it can be seen that the estimate is similar to the current estimate of the WGR, however, the estimate for the period of 28 days differs a lot from the current estimate for well PD08. In Appendix B it can be observed that for PD10 the estimate of this period is a bit larger, which explains the small error for also this period.

3.2.2 Comparison water production

The measured water production compared to the estimated water production can be found in Figure 3.3, when the WGR is assumed constant for 28 days.

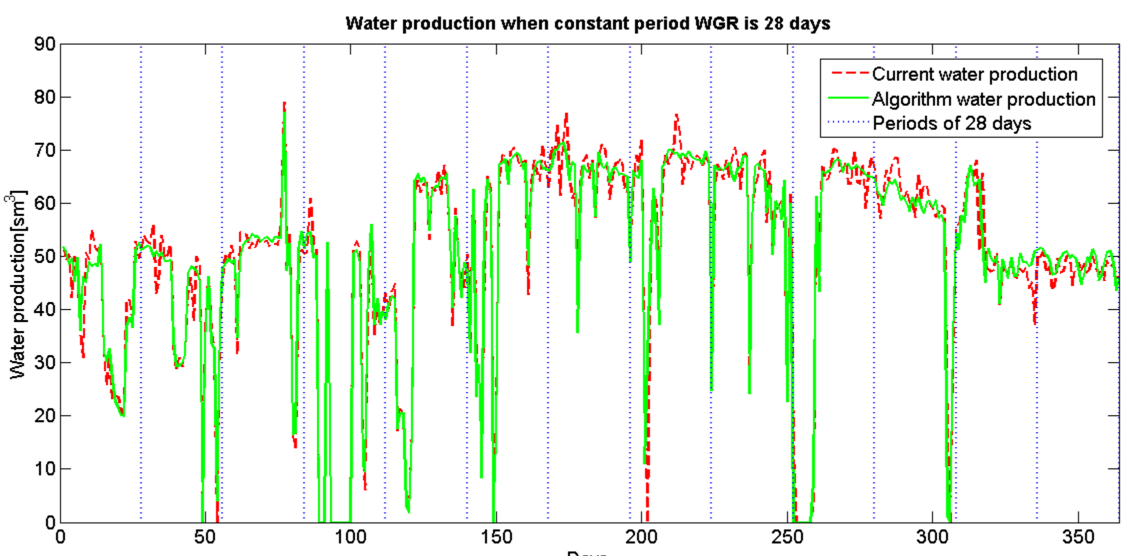

FIGURE 3.3. Water production estimated and measured, WGR kept constant for 28 days

From Figure 3.3 it can also be concluded that the algorithm works quite well. On some places a significant difference between the estimated and measured water production can be seen, but overall both are similar.

A closer look at the measured and estimated amount of produced water is given in Figure 3.4.

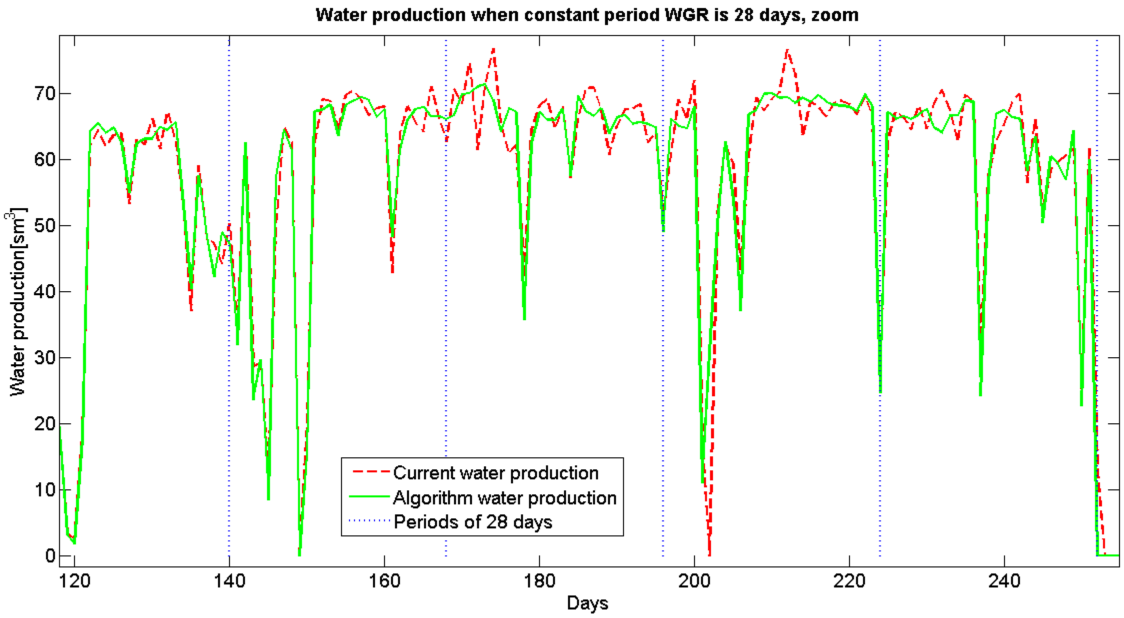

FIGURE 3.4. Water production estimated and measured, WGR kept constant for 28 days, zoom

The figure shows that especially at large changes in the water production, the algorithm follows this trend precise. But when the water production remains stable, the algorithm behaves less exact. This can be explained from the fact that WGRs are assumed constant for a certain period. At the sudden changes, the algorithm makes the largest error of the whole period. Therefore, is the water production best estimated by the algorithm at those days at the expense of the other days in the period. Also notice that when the water production suddenly decreases, the algorithm is over-correcting (around day 160 and 225 for example); the water production is too large compared to the measured water production. This is counter-intuitive but it is very dependent on the gas production data; if the gas production data is not showing this behaviour, it is difficult for the algorithm to reconstruct this behaviour for the water production. There are some days on which either the water production or the gas production or both show such capricious behaviour.

A solution to handle this behaviour might be to take these days not or less into account than days on which the behaviour is more fluent compared to the previous day(s). This can be done by weighted LSM, where each day is marked with a weight indicating how much that day is 'weighted' during the estimation process. However, the amount of days where this should be implemented is quite a lot which makes the process cumbersome. Moreover, this behaviour is characteristic for the problem and thus the model should be able to deal with it.

3.2.3 Algorithm performance

During the construction of a model, it is important to investigate the performance of the model in terms of usage. Therefore, below information is given about the number of iterations (Figure 3.5) and the computation time (Table 3.2).

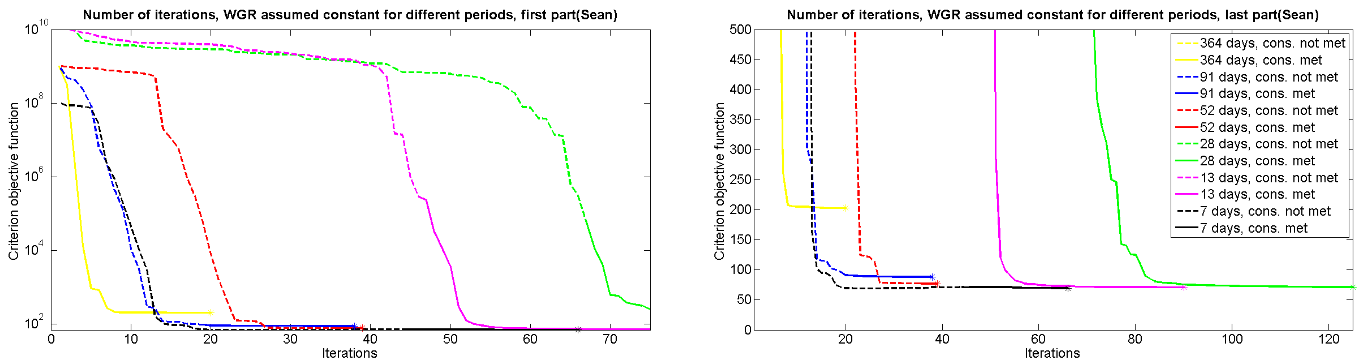

FIGURE 3.5. Iterations and value objective function, Sean PD platform

The figures above show the number of iterations and the value of the objective function. The left figure shows the first part of the iterations where the largest decrease is shown, notice that a log scale is used here. The dashed line means that the equality constraints are not met, which is the case when the line is solid. The asterisk indicates the total amount of iterations until the minimum of the objective function is reached while the constraints are met. As explained before, the solution is very dependent on the initial guess of the WGRs. The periods have a different initial guess, explaining the different initial function values. This may also be the reason that a smaller period (and thus more variables to be estimated) does not mean more iterations are needed compared to a longer period. For example, when $T = 7$ days, the algorithm reached the minimum in less iterations than when $T = 13$ days.

Table 3.2 contains an overview of other characteristics of the simulation run to find estimates of the WGR.

WGR constant for	**WGRs** (=5*Periods)	**Iterations** (Iter. until const. met)	**Function evaluations**	**Run time(s)**
364 days	5	19(1)	114	0.173242
91 days	20	37(20)	859	0.529321
52 days	35	38(36)	1434	0.738204
28 days	65	124(68)	8296	4.668100
13 days	140	89(47)	12756	9.840818
7 days	252	65(45)	17342	21.176901

TABLE 3.2. Characteristics of the model performance, Sean PD platform

The second column of Table 3.2 indicates the number of variables that needs to be estimated. The third column shows the number of iterations until the algorithm reached its minimum, where the number in between brackets shows when all constraints were met for the first time. The fourth column shows the amount of function evaluations needed, which the algorithm needs to check in what direction the decrease in the objective function is the largest. The last column indicates the time needed to run the algorithm. What can be noticed is that the period with the largest amount of WGRs, does not need the most iterations to converge. However, the run time is the largest for this period which is caused by the large amount of function evaluations. An explanation for the first comment can be found in the initial guess for this period and thus large initial value of the objective function. A rule of thumb for the maximum amount of iterations needed for an optimization problem (if it is well-posed) is that this should be equal to the amount of variables +1. This is only reached for the two smallest periods. This might be caused by the size of the WGRs. These are very small ($10^{-5} - 10^{-6}$) which means that the algorithm spends a lot of iterations on finding the local minimum. Another possible cause for the large number of iterations, can be the high starting point of the objective function.

3.3 Conclusion

This chapter a model is constructed for the Sean area, which has five wells. The estimated WGRs are realistic; non-decreasing and for different wells of the same order. A relative error of 5% is made, which is small. This error can be caused by measuring errors, which are not taken into account, or by time delays, which are assumed not to be present here.
Although the algorithm performs well, there are also some remarks. The estimated WGR is very dependent on the initial guess. Also the algorithm needs more iterations than expected. This can be caused by the previous comment or the fact that the WGRs are very small, hence resulting in a lot of computational effort to find the local minimum.
Hence, for this small area it is possible to construct a model that constructs realistic WGRs. The next chapter investigates if this is also possible for a larger area.

Chapter 4

Extending the model

This chapter aims to model the more complicated area, Solepit, such that realistic WGRs can be estimated with a small difference between the measured and estimated water production.
This chapter will first study the Solepit area. After that the available data and the current WGRs are considered. The additional complexities of Solepit are explained, after which the results are discussed.

4.1 Solepit area

This chapter looks at a larger area, the Solepit area. A picture of the area and its details about the pipelines (length and cross section) can be found in Appendix A. Figure 4.1 shows the flows of the platform.

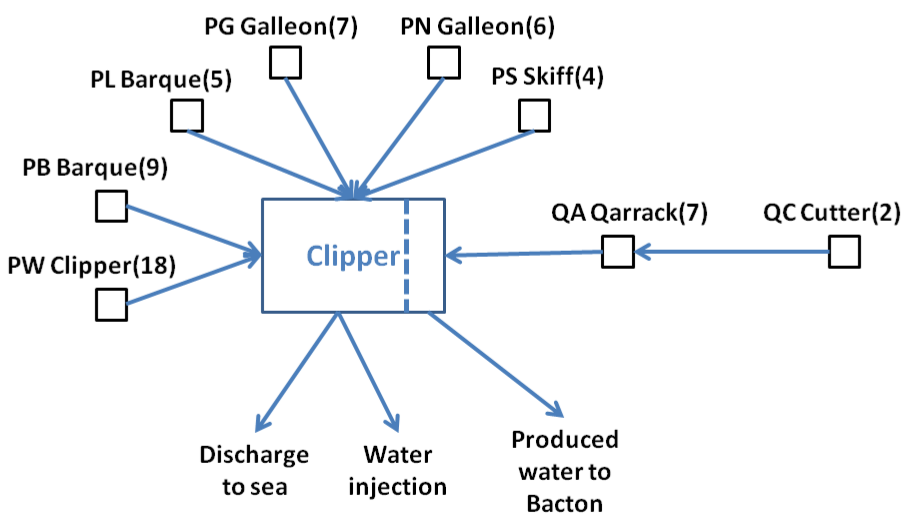

Figure 4.1. Gas and water flows at the Solepit area offshore

The number in between brackets indicates the number of wells operated from each satellite platform. Notice that at Solepit we are dealing with 58 wells, compared to the 5 producing wells at Sean. The water that is produced by the wells Cutter and Qarrack is transported to Bacton immediately, such that there are 49 wells left of which the WGR is being estimated.

Also note that in the Solepit more satellite platforms are present than there are in the Sean area. More importantly, there are more gas fields present in this area. This means that it is harder to notice trends, if this is possible for the fields; every gas field is different (for example the contour of the gas layer as illustrated in the first chapter in Figure 1.2) and wells are designed differently (for example the angle or the depth of the well). This is also the reason why a larger gas production does not imply that the water production is larger. This makes it impossible to allocate the water relatively to the total gas production and indicates why a model is more suitable for this problem.

4.2 Data

Also for the Solepit area it holds that from all wells the gas production is known and from all these wells together the water production is known. To get an indication of the size of these numbers, Figures 4.2-4.5 can be used. First Figure 4.2 gives an overview of the available data.

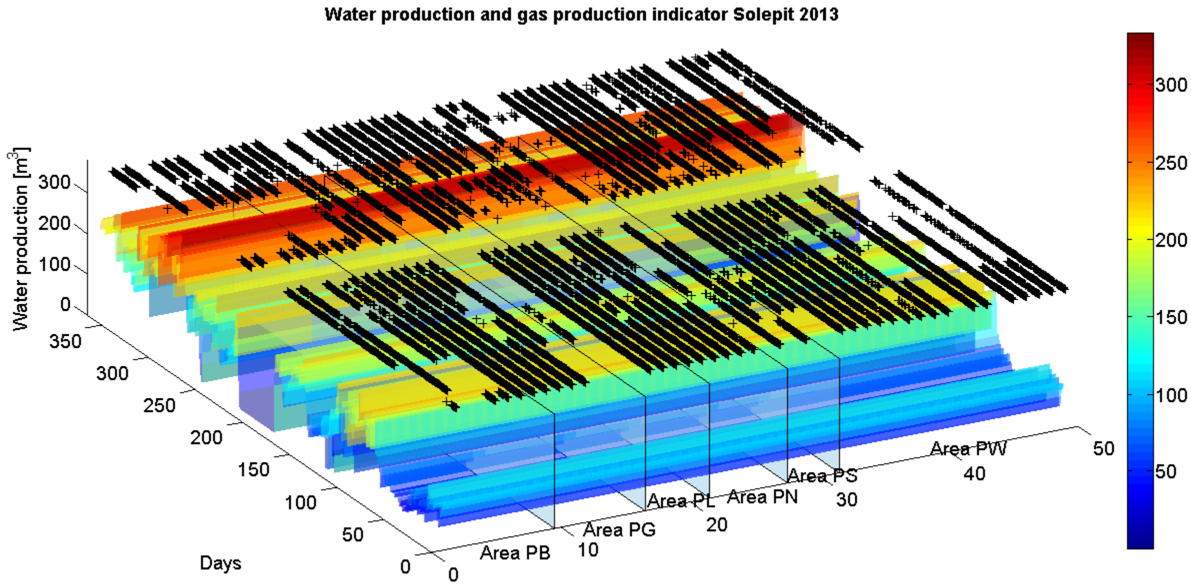

FIGURE 4.2. Gas and water production Solepit area

The figure shows the water production (z-axis) over the year (y-axis) for all wells (x-axis) together. The plusses on top of the figure indicate that a well was producing on that day. The intersections show the satellite areas and their wells.

Figure 4.3 contains the topview of Figure 4.2 and gives a better view of the size of the water production over the year.

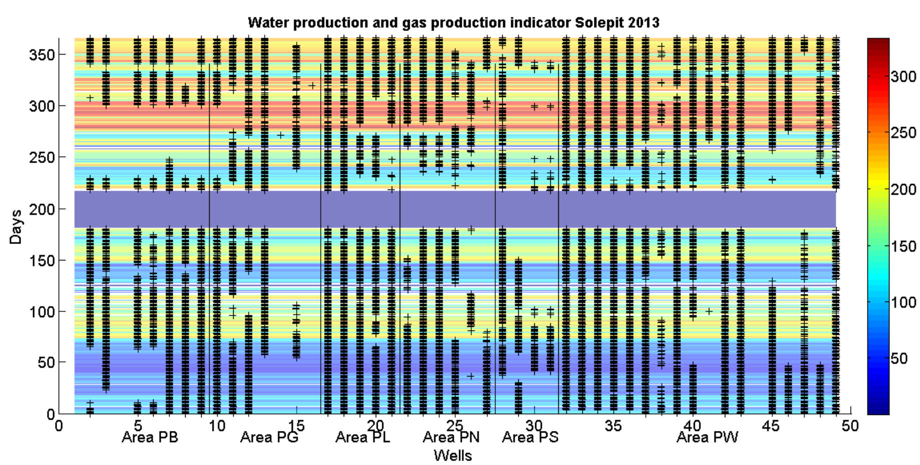

FIGURE 4.3. Water production Solepit area

The data shows that there is a shutdown of approximately a month around day 200 of the year. After that period the wells produce the highest amounts of water (probably (partially) caused by the sweep-phenomenon which will be discussed in detail later on). It can also be seen that wells 1,4,13,15 and 39 have no gas production on (almost) all days of the year. Lastly, the black lines indicate the six satellite platforms of Solepit.

Figure 4.4 and 4.5 show the gas production of the Solepit area and give more insight in the size of this production. The first figure shows the gas production per well and the second figure the total production per platform within the Solepit area.

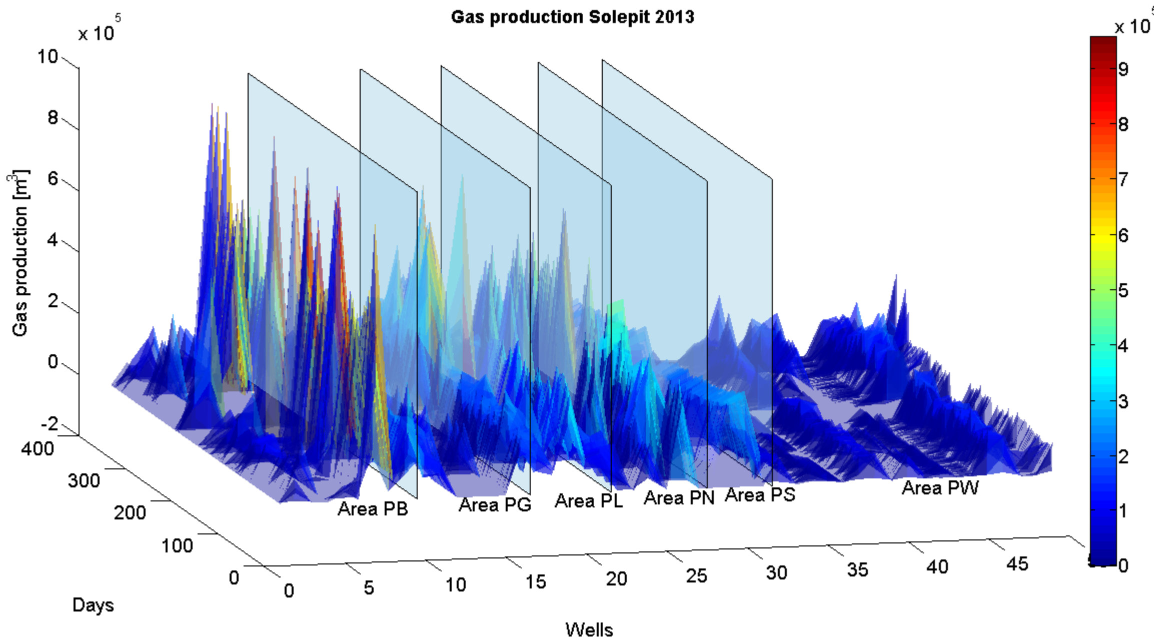

FIGURE 4.4. Gas production per well Solepit in 2013

It can be seen from Figure 4.4 that there are large differences in the gas production throughout the year and per well. There are only a few wells that have a large gas production, whereas the majority of the wells produces a smaller amount. The consequences for the production per platform can be seen in Figure 4.5.

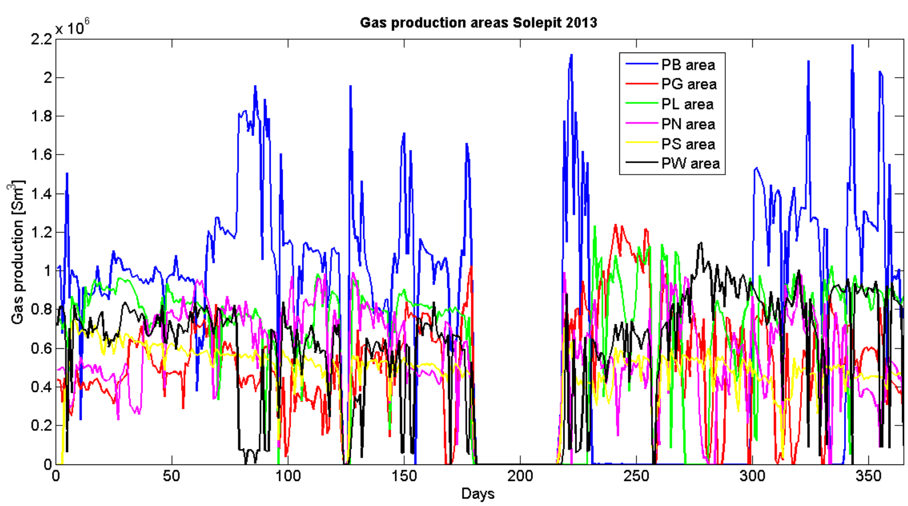

FIGURE 4.5. Gas production Solepit per platform in 2013

The above figure shows that also over the year the PB platform has the largest gas production. The other platforms produce gas at roughly the same rate. Some are fluctuating a lot from zero to any size (PW), while other areas have a gas production through the whole year (PN); accept for the period from day 175-225 where none of the wells are producing gas. Keep in mind that although the PB platform produces more gas than the other platforms, this does not imply that it will also produce the largest amount of water. This is dependent on a lot of factors, as explained earlier in this chapter (section 4.1).

Now that the gas production has been investigated from several angles, the water production can be studied. Figure 4.6 shows the water production over the year in combination with the gas production of all wells together.

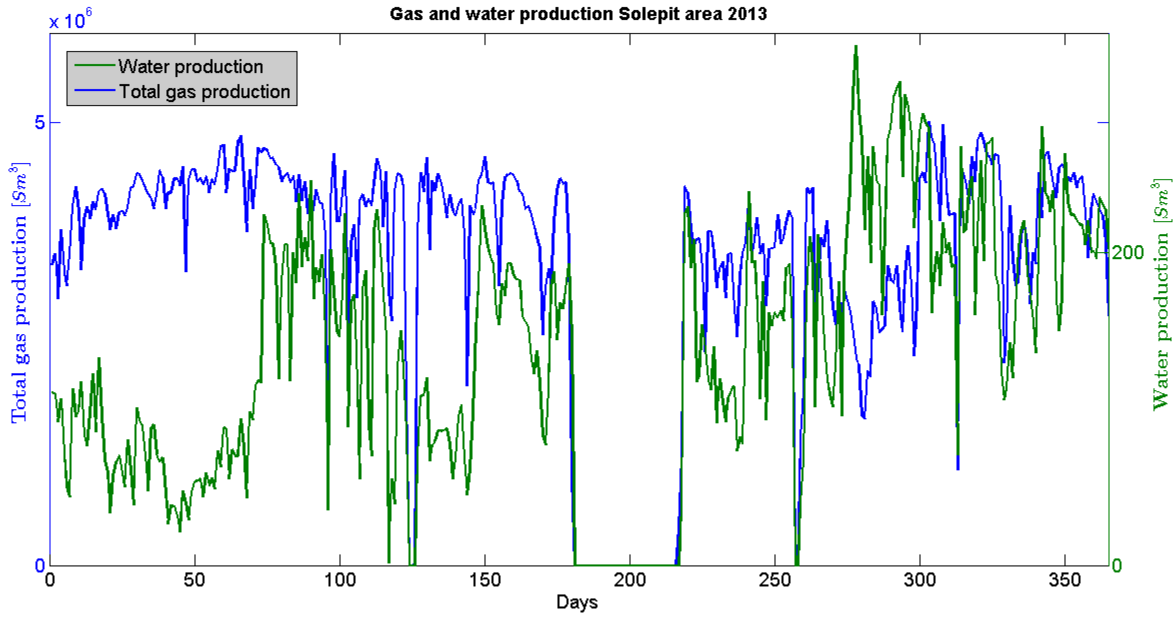

FIGURE 4.6. Water and gas production Solepit 2013

A similar figure at the Sean area gave a lot of insight in the expected behaviour of the WGR (Figure 1.3). However, from the above figure almost no conclusions can be drawn. This is mainly caused by the large amount of wells and gas fields that are responsible for the total gas production. This figure might indicate that there is a possible delay in the water production, because the behaviour of the water production does not mimic the behaviour of the gas production. This is expected since the gas production influences the water production.

4.3 Current WGRs

The current WGRs of satellite platform PL of the Solepit area will be discussed in this subsection. The WGRs of the other platforms can be found in Appendix C. Figure 4.7 shows the behaviour of the current estimates of the five wells at the satellite platform PL.

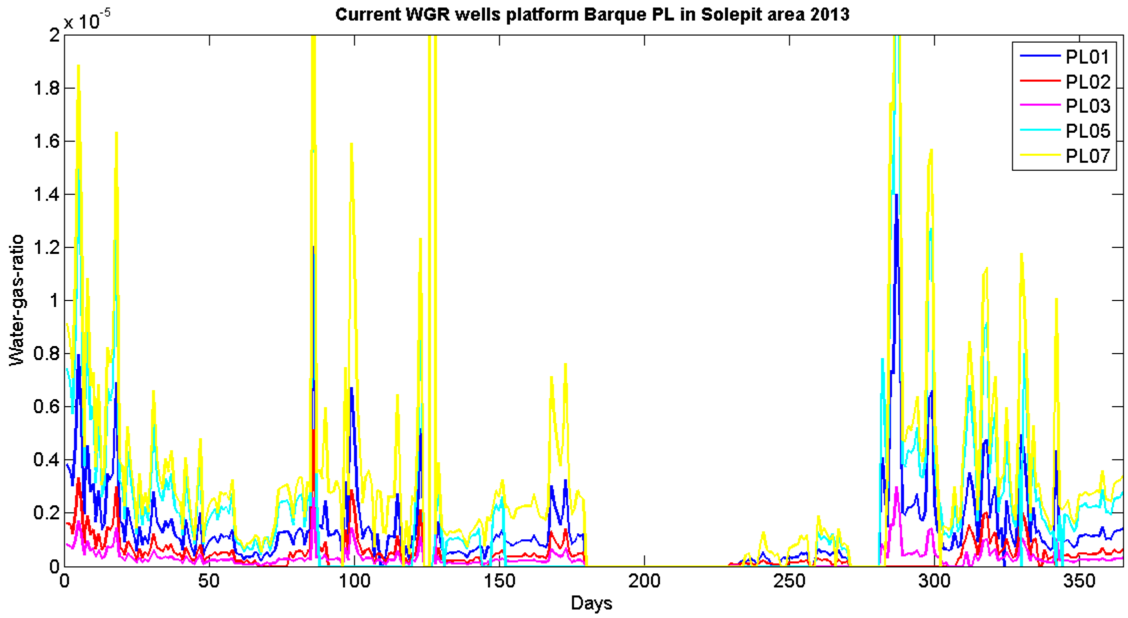

FIGURE 4.7. Current WGR estimates PL platform, Solepit area 2013

The figure shows large differences in the size of the WGR between the wells. Furthermore, it can be seen that the WGR changes quickly for all wells, but PL07 in particular. As expected, no clear trend in the behaviour of the WGR can be seen. The large peeks in the WGR are not realistic, considering the physical meaning. One could think that this behaviour is caused by the consequence of a break-down as explained in the first chapter. Hence, in Figure 4.8 the gas production and current WGR estimate of PL07 are shown. And for a clearer view of the behaviour at the peaks, Figure 4.9 contains a zoom around two peaks.

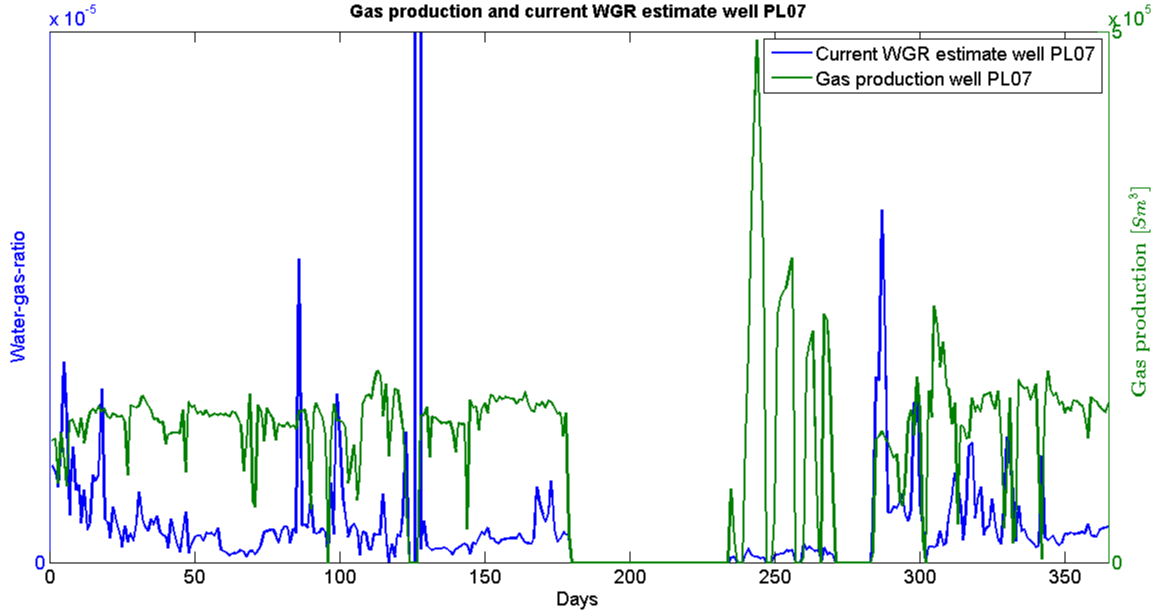

FIGURE 4.8. Gas production and current WGR estimate well PL07

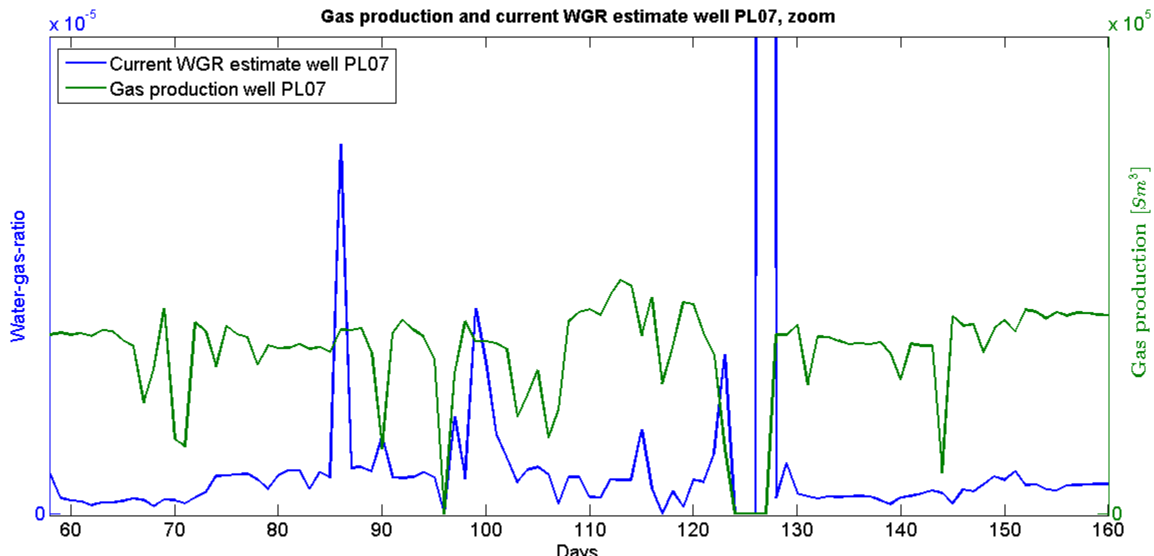

FIGURE 4.9. Gas production and current WGR estimate well PL07 zoom

From the figures no clear relation considering the peaks can be seen. This means that no physical relation between the gas production and the WGR is present. The large peaks, some peaks were also seen at the Sean area, are most probably errors in the current allocation model and should not be focused on during the estimation process.

This unrealistic behaviour of the current estimates means that it is hard to compare the results of the model to these numbers. At the Sean area this was possible, since the main model was only lacking non-decreasing WGRs but an increasing trend was visible. But for the Solepit area, no clear trend can be noticed which means that the estimated WGRs of our model will be very different from the current estimates.

4.4 Details of Solepit

These are the points of attention which need to be implemented additional to the basic model:

1. Sweep
2. Time delay
3. Uncertainty
4. Additional constraint

These will be discussed in detail in this subsection.

4.4.1 Sweep

The water, dissolved in the natural gas, condensates in the pipelines. Since water is heavier than gas it sinks to the bottom of the pipeline. The velocity of the water is thus smaller than the velocity of the gas, however, the second does influence the first since it flows right above it. This means that during a period of small or without production, the amount of water in the pipeline increases. As soon as the gas production is increased to its normal values, this accumulated water is produced in addition to the water production of the current gas production. This phenomenon is called sweep.

It is also stimulated by the fact that during a shutdown the pressure increases as a result of the accumulation of the gas, causing the velocity of the gas, and thus of the water, to increase even more. An example of this sweep phenomenon most probably occurred after the shutdown of a month in 2013, which was seen in Figure 4.3.

For our problem this sweep phenomenon means that the WGR increases shortly after the shutdown but then needs to decrease. However, the algorithm currently has constraints that prevent the WGR to decrease over the year. In addition, the pipelines at the Solepit area are larger than at the Sean area such that more water accumulates and the sweep plays a more significant role (Heitman, 2014b). Thus the WGR-non-decreasing constraint will be adapted such that after a shutdown (a well which produces no gas for at least one day), the non-decreasing constraint will be dropped for a certain number of days. However, this is very complicated to implement because the length of a shutdown influences the amount of days this constraint should be neglected. Not enough information is available, but if more information on this topic is gained this should be implemented.

4.4.2 Time delay

Time delay is defined in this context as a time difference between the time at which the water/gas production was measured and when it was produced real time. This is especially important if the time delay for the water and gas production is different, meaning that this delay should be taken into account.

In chapter 3 it could be assumed that there was no time delay present, because distances between the platforms at the Sean area were very small. For the greater Solepit area these distances are larger. It is expected that this causes delays. This can also be seen in the data, because there are days where there is a gas production but no water production. However, the same phenomenon was noticed at the Sean area.

It is most likely that the gas production does not contain delays. The delay in the water production on the other hand is hard to define. There might be an influence from the length of the pipeline, which means that more water is collected in these lines, meaning that the rate of influence of the sweep phenomenon increases. The velocity of the gas (which is mainly causing the sweep) is regulated by the pressure in the pipelines.

For every pipeline the relation between the pressure and the amount of water that accumulates in the pipeline is known. The pressures in the wells are unfortunately not available. However, if they were, it would still be quite some work to use this information to find the 'true' water production. Every platform(pipeline) has its own delay, which is monitored every hour. This means that one platform can have a delay of one day and the other platform two days. Still, the total water production as it was measured needs to be produced by all these platforms if the delay is taken into account. Although it might be cumbersome, it is definitely something that needs to be considered to increase the accuracy of the model.

4.4.3 Uncertainty

The data contains some uncertainty, in the form of wrong data, missing data and inaccurate measurements. The first two occur by indicating that there is gas or water production, while this is actually not the case or the other way around. This is difficult to incorporate in the model and will therefore be neglected. However, if the results show strange behaviour one should not forget that this might occur due to this phenomenon.

Implementing inaccurate measurements on the other hand, is possible in the model. Both the gas and water data are inaccurate as explained in section 2.2.2. The gas numbers have an uncertainty of 10% (variance of the measurement is equal to this number multiplied by the gas production) and the water numbers have an uncertainty of 20% (variance of the measurement is equal to this number multiplied by the water production). This has the following consequences for the variables in the minimization problem:

$$(G^i_j)_{used} \sim \quad N((G^i_j)^{meas}, 0.1(G^j_i)^{meas}) \qquad \forall j \in \{1,\ldots,n\}, \forall i \in \{1,\ldots,N\} \tag{26}$$

$$(w_j)^{used} \sim \quad N((w_j)^{meas}, 0.2(w_j)^{meas}) \qquad \forall j \in \{1,\ldots,n\} \tag{27}$$

Hence, the matrix $\widetilde{G}_j$ and vector $\widetilde{w}_j$ contain then the values $(G^i_j)^{used}, (w_j)^{used}$. The uncertainty is taken into account as described in section 2.2.2. The uncertainty will be applied at the end, when the model for the Solepit area is constructed (section 4.6).

4.4.4 Additional constraint

As explained in chapter 2, a constraint is added to ensure that the model gives realistic estimates of the WGR. Where for the Sean platform realistic estimates were easily defined, for the Solepit platform this is more complicated. At the Sean platform there are only a few gas fields, while at the Solepit platform there are many. Therefore, it is harder to notice trends since the gas originates from different gas fields. Thus, the production programmer needs to use well tests to gain more insight in realistic values for the WGR. These tests result in very accurate measurements of specifics of a well. However, they are expensive, and therefore not executed frequently. An overview of the results of the most recent well test for the Solepit area can be found in Appendix D. These results will be discussed here to formulate the additional constraint for the Solepit platform.
Note that this well test is the most recent well test performed in 2014, while the gas and water data from Solepit are from the year 2013. For Sean area it was observed that the WGRs double in a year time. Thus, the numbers about the WGRs of the well test from the year 2014 are halved as an estimate for the well test numbers from 2013.

From Table D.7 in Appendix D it can be concluded that there are some wells with a significant larger WGR compared to the other wells. This measured WGR will be used as a lower bound for these wells in the algorithm. Notice furthermore that the other wells, with a WGR larger than 1 ([bbl/MMscf]=[barrel/ million standard cubic feet], which means the amount of barrels water produced per million standard cubic feet gas produced), all differ at most a factor 10. Therefore an additional constraint is added, which relates the WGRs of all these wells together, with a maximum difference of a factor Δ set equal to 10. This results in the following adapted/additional constraints (the order of the wells is changed such that now all wells with no significant size come first and after that all wells with a WGR of significant size):

$$-\frac{1}{\Delta}\widetilde{r}^{k}_{(i-1)N+1:iN} \leq \widetilde{r}^{m}_{(i-1)N+1:iN} \leq \Delta\widetilde{r}^{k}_{(i-1)N+1:iN} \quad i \in \{1,\dots,Q\}, \quad m \in \{1,\dots,N_{nw}\} \quad k \in \{1,\dots,N_{nw}\}\backslash\{m\} \tag{28}$$

$$\widetilde{r}^{m}_{i} \geq 0 \quad i \in \{1,\dots,Q\}, \quad m \in \{1,\dots,N_{nw}\} \tag{29}$$

$$\widetilde{r}^{l}_{i} \geq \text{WGR}^{*}_{m} \quad i \in \{1,\dots,Q\}, \quad l \in \{N_{nw}+1,\dots,N_{nw}+N_{w}\} \tag{30}$$

where N_w is the amount of wells with a WGR of significant size, N_{nw} is the amount of wells for which this does not hold and is thus equal to $49 - N_w$. This means that all N_{nw} wells have a total amount of $N_{nw} - 1$ constraints.
First equation (29) applied to all wells, now it only applies to the N_{nw} wells. The N_w wells on the other hand have the measured WGR from the well test, which is indicated by WGR_m, as a lower bound. Note that this value was halved, indicated by WGR^*_m, to compensate for the fact the well test is from 2014 while the data is from 2013.

This results in the following mathematical model:

$$\min_{\widetilde{r}} \quad ||\widetilde{\varepsilon}(\widetilde{r})||_2 \tag{31}$$

$$s.t. \quad -\tfrac{1}{\Delta}\widetilde{r}^{k}_{(i-1)N+1:iN} \leq \widetilde{r}^{m}_{(i-1)N+1:iN} \leq \Delta\widetilde{r}^{k}_{(i-1)N+1:iN} \quad i \in \{1,\dots,Q\},\ m \in \{1,\dots,N_{nw}\} \quad k \in \{1,\dots,N_{nw}\}\backslash\{m\} \tag{32}$$

$$\widetilde{r}^{m}_{i} \geq 0 \quad i \in \{1,\dots,Q\},\ m \in \{1,\dots,N_{nw}\} \tag{33}$$

$$\widetilde{r}^{l}_{i} \geq \text{WGR}^{*}_{m} \quad i \in \{1,\dots,Q\},\ l \in \{N_{nw}+1,\dots,N_{nw}+N_{w}\} \tag{34}$$

In Appendix D the WGRs for which a value of significant size was measured, are divided in three groups:

(1) WGRs which are much larger than $1-10$(the WGR of most wells), indicated by a green colour.
(2) WGRs which are larger than $1-10$, indicated by a yellow colour.
(3) WGRs which are a bit larger than $1-10$, indicated by a blue colour.

There are three possible options for the value of N_w: either only the green wells can be taken ($N_w = 4$), or the green and the yellow wells ($N_w = 6$) or the green, yellow and blue wells ($N_w = 8$).

4.5 Results

This section contains the results for the Solepit area. Here only the situation is discussed when four wells are assumed to have a lower bound based on the results of the well test (N_w=4 and thus $N_{nw} = 45$). The results for well PS01 can be found in Figure 4.10. This is a well which did not have a significant size for the WGR in the well test and thus had a WGR of order 1, one of the N_{nw} wells. The results for well PB11 can be found in Figure 4.11. This well did have a measured WGR of significant size during the well test, one of the N_w wells.

Note that, due to computational limits, from now on only the four smallest periods (T=364, 91, 52, 28) over which the WGR is assumed constant, are considered.

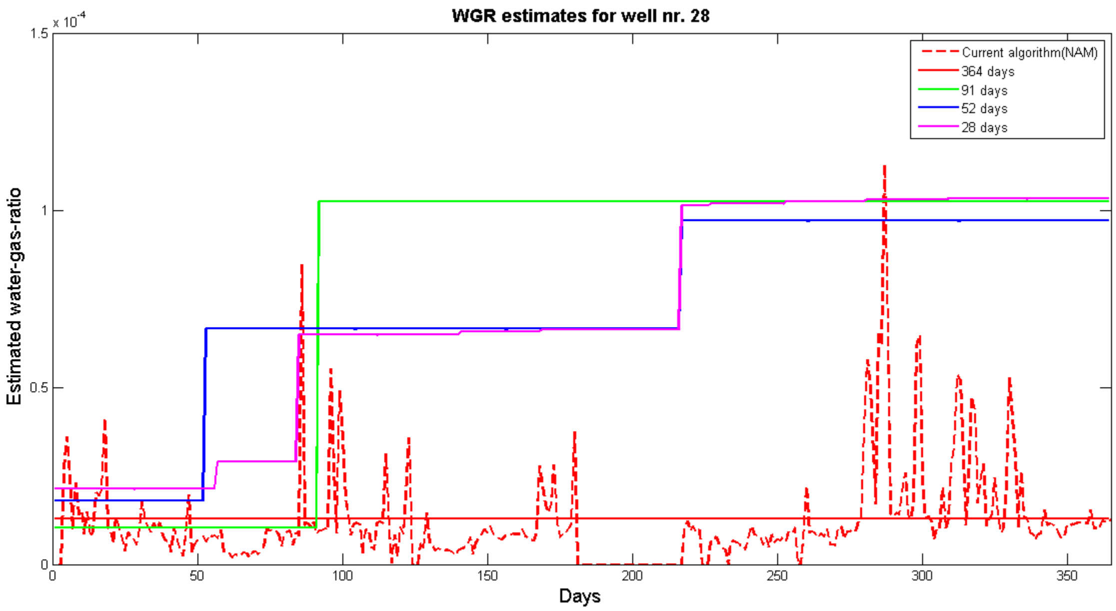

FIGURE 4.10. WGR assumed constant over different periods, well PS01 (four wells having a lower bound based on well test)

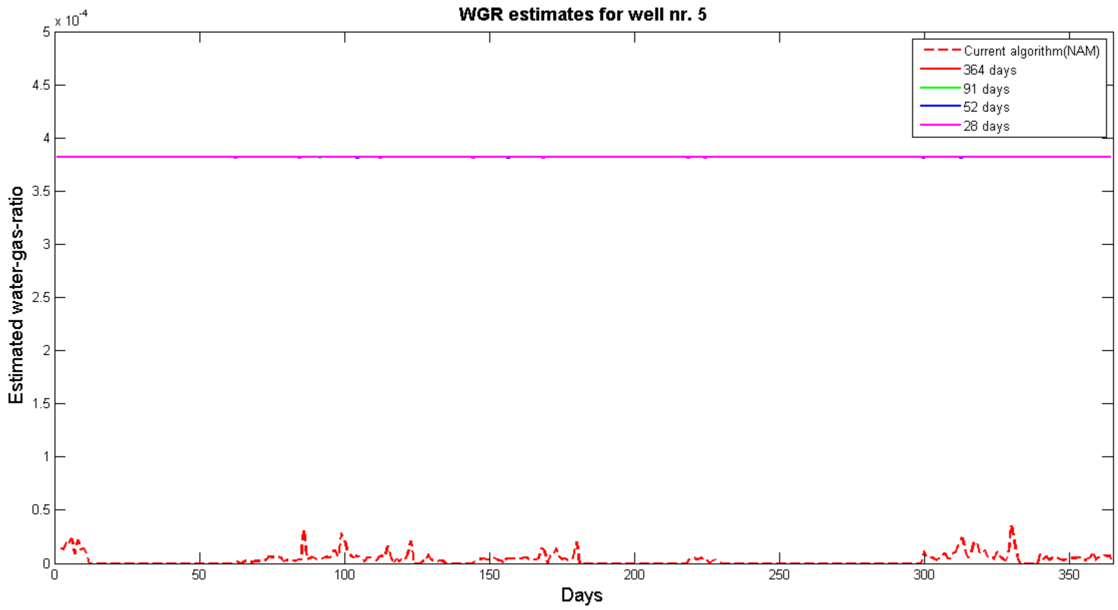

FIGURE 4.11. WGR assumed constant over different periods, well PB11 (four wells having a lower bound based on well test)

The WGR of well 28 is of similar size as the current estimate, but has increasing behaviour. The WGR of well 5 other hand is much larger than the current estimates, equal to the lower bound which is based on the results of the well test. Note that the WGR remains constant over the year for all periods. This is most probably due to the lower bound which is constant over the whole year. Apparently the model first estimates the four wells which have a significant size and then uses the other wells to find the smallest error.
At the Sean area the solution was very dependent on the initial guess of the WGRs. This phenomenon was not seen here. An explanation is that the periods $T = 13, 7$ are not simulated here, the periods where this phenomenon was mainly seen. Another explanation can be found from the fact that the current estimates of the WGR do not imply a clear improved WGR which does meet the non-decreasing constraint. Hence, the solution set for this area is smaller than the solution set in the Sean area.
In Appendix E the results for these wells can be found if more wells were given a lower bound based on the results of the well test ($N_w = 4 + 2 = 6$ or $N_w = 4 + 2 + 2$).

4.5.1 Error analysis

Table 4.1 contains the errors belonging to the simulation run.

WGR constant for	2-norm error	Relative error
364 days	947.8396	28.31%
91 days	843.2986	24.53%
52 days	854.8994	24.92%
28 days	827.0151	23.72%

TABLE 4.1. 2-norm and relative error Solepit algorithm (four wells having a lower bound based on well test)

Table 4.1 shows that the 2-norm error is large. Also the relative error is large with a value of around 25%. Note that both the 2-norm and the relative error hardly decrease if the WGR is assumed constant for either 91 or 52 or 28 days.

4.5.2 Comparison water production

This section shows the water production estimated by the model and the measured water production. Figure 4.12 contains these values over the whole year, while in Figure 4.13 a zoomed version of a part of the year is given.

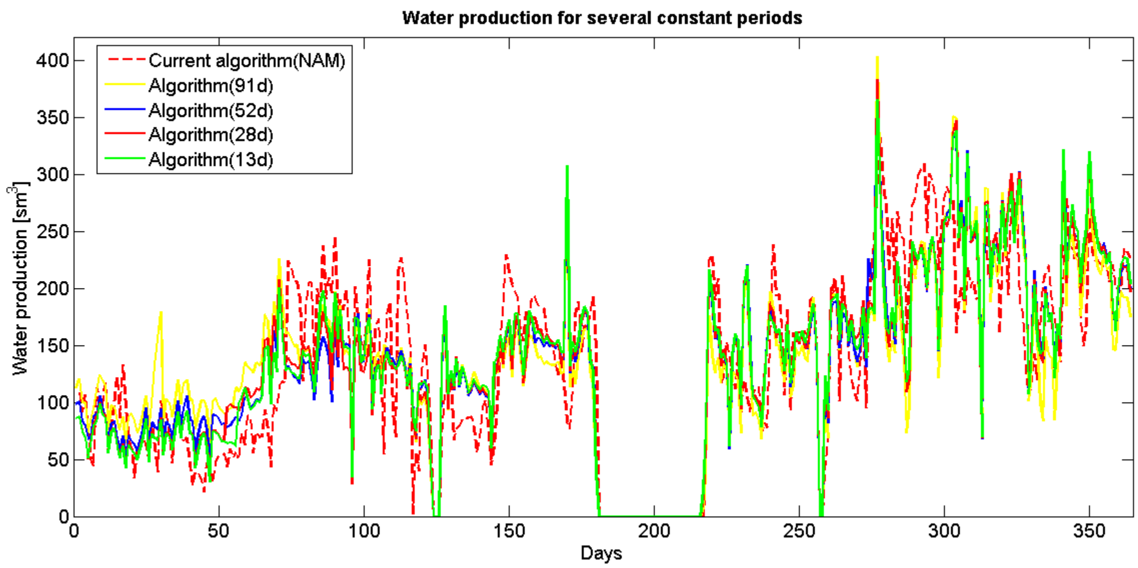

FIGURE 4.12. Water production estimated and measured, WGR constant for different periods

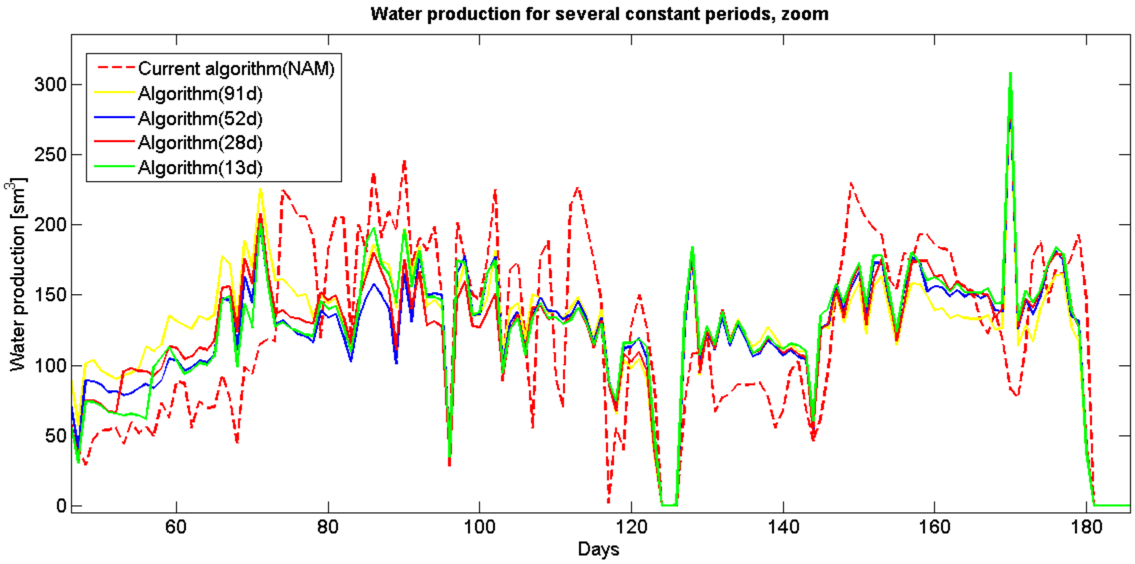

FIGURE 4.13. Water production estimated and measured, WGR constant for different periods, zoom

From the figures it can be seen that none of the periods over which the WGR is assumed constant, follows the measured water production accurately. On some days the estimated water production is accurate. In Figure 4.13 there can even days be noticed where the measured water production decreases and the model produces an increasing water production (for example at approximately day 170). This might come from the fact that the WGR is assumed constant for a longer period. If at that day the gas production is small, the error is automatically also small (remember $\widetilde{\varepsilon}_i = \widetilde{w}_i - \widetilde{G}_i \widetilde{r}_i$). Resulting in less accurate estimates on that day, such that the errors on the other days in the same period are minimized.

4.5.3 Model performance

Below the model performances are discussed in terms of iterations and computation time. Figure 4.14 contains the value of the objective functions plotted against the number of iterations.

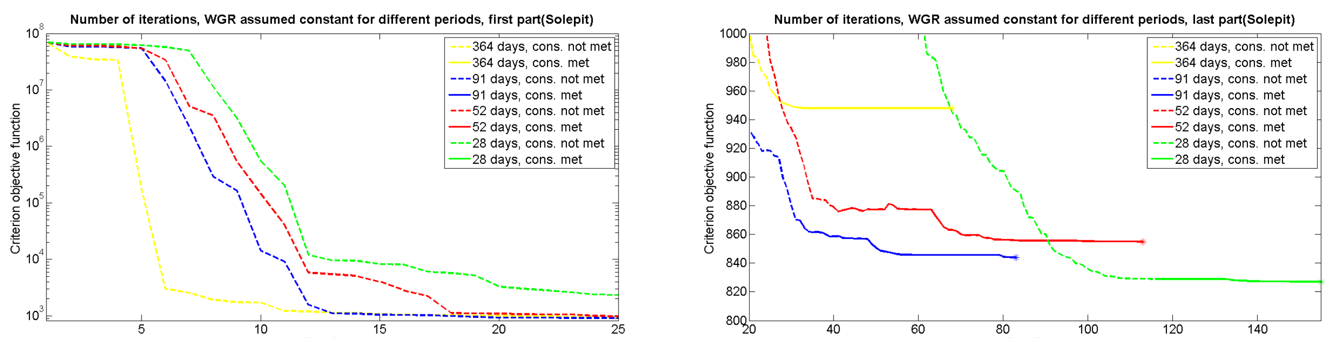

FIGURE 4.14. Iterations and value objective function, Solepit platform

The figure on the left contains the first 25 iterations, where the largest decrease in the objective function is obtained. Note that a log scale is used here. The figure on the right shows the iterations where the decrease in the objective function is only small. The dashed line indicates that the constraints are not met, which is the case when the line is solid. The asterisk in the right figure indicates the end of the simulation, when the minimum of the objective value is reached. From the figures it can be concluded that the more WGRs that have to be estimated, the more iterations are needed to reach the minimum of the objective function. This was not seen at the Sean platform, however, there different initial guesses were used for the periods which is not the case here. Table 4.2 contains characteristics about the performance of the model.

WGR constant for	**WGRs** (=49*periods)	**Iterations** (Iter. until const. met)	**Function evaluations**	**Run time(s)**
364 days	49	67(26)	3490	8.918361
91 days	196	82(30)	16436	30.656760
52 days	343	112(41)	38995	98.979131
28 days	637	154(117)	98940	364.551855

Table 4.2. Characteristics of the model performance, Solepit platform

The rule-of-thumb says that the amount of iterations should be less or equal to the amount of variables +1. This rule is violated for the first period. The other characteristics are as expected; if the amount of periods increases, the iterations and the run time increase. Note that the model runs for a long time if the WGR is assumed constant for 28 days. To gain estimates where the uncertainty is incorporated as well, the model has to be run for several times (at least more than 20 to determine 95%-confidence intervals). With a computation time of approximately six minutes for one run, this total run time will be large.

4.5.4 Conclusion

In this last section, a model was constructed for the Solepit area, where the uncertainties were not taken into account yet. To ensure realistic WGRs, the well test was used as a lower bound for some of the wells. The model estimated these WGRs constant over the whole year. For wells with no lower bound, the WGRs show increasing behaviour which obviously differs a lot from the current estimates. The model makes a relative error of $\approx 25\%$, which is large. This might be caused by the implementation of the well test. Another cause can be that the delay was not incorporated in the model, because although a lot of information is known about it, it is too difficult to understand the exact structure. Furthermore, the run time of the model is long. This model will be used as the final model where the error in the measurements are implemented to find 95%-confidence intervals of the WGRs.

4.6 Complete model with uncertainty

Now that the model is known, the uncertainties will be incorporated in the model as explained in section 4.4.3: both the water and gas production numbers contain uncertainties. The variance of the water production numbers is used in the calculation of the weights during the application of weighted LSM. The model is run 50 times where the WGR is assumed constant for 364, 91, 52 and 28 days. Every run a different combination of gas and water production numbers is drawn from the normal distribution as given in section 4.4.3.

The 95%-confidence intervals for two of the 49 wells can be found in Figure 4.15-Figure 4.18 and Figure 4.19. First the results for well PS01 are given (no significant size WGR in well test) and secondly for well PB11 (significant size WGR in well test).

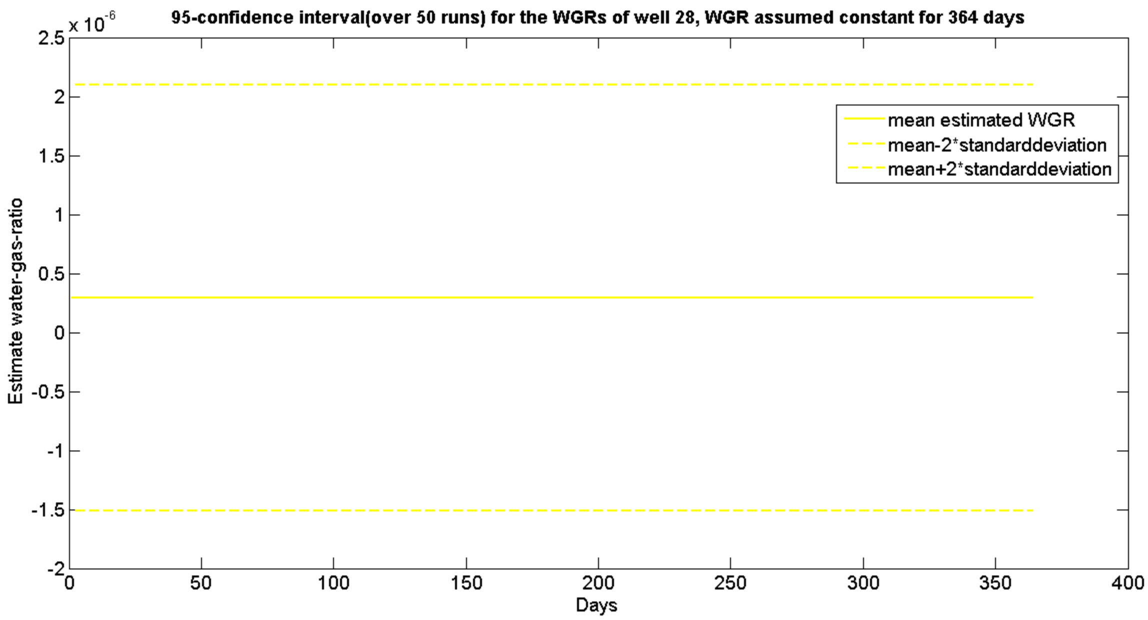

FIGURE 4.15. 95%-confidence intervals WGR (assumed constant for 364 days), well PS01

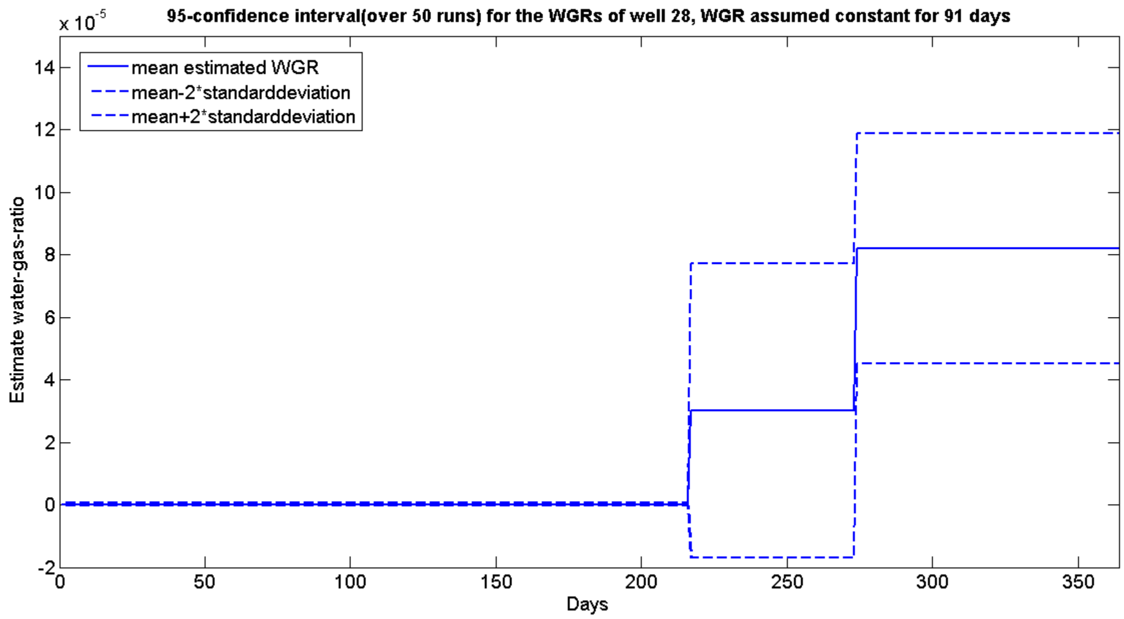

FIGURE 4.16. 95%-confidence intervals WGR (assumed constant for 91 days), well PS01

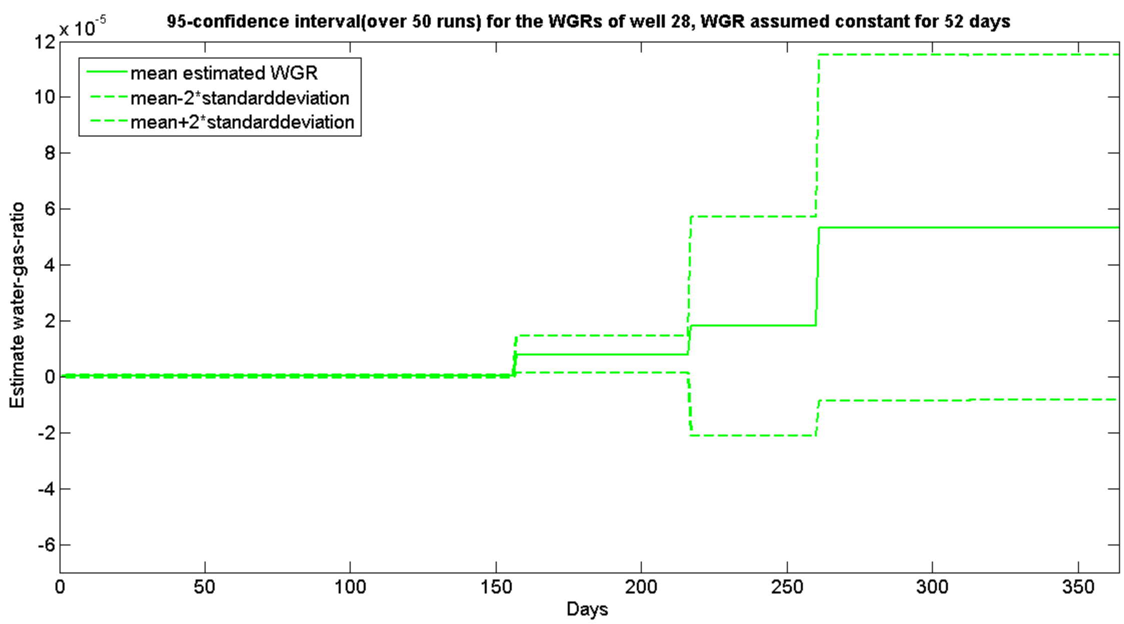

FIGURE 4.17. 95%-confidence intervals WGR (assumed constant for 52 days), well PS01

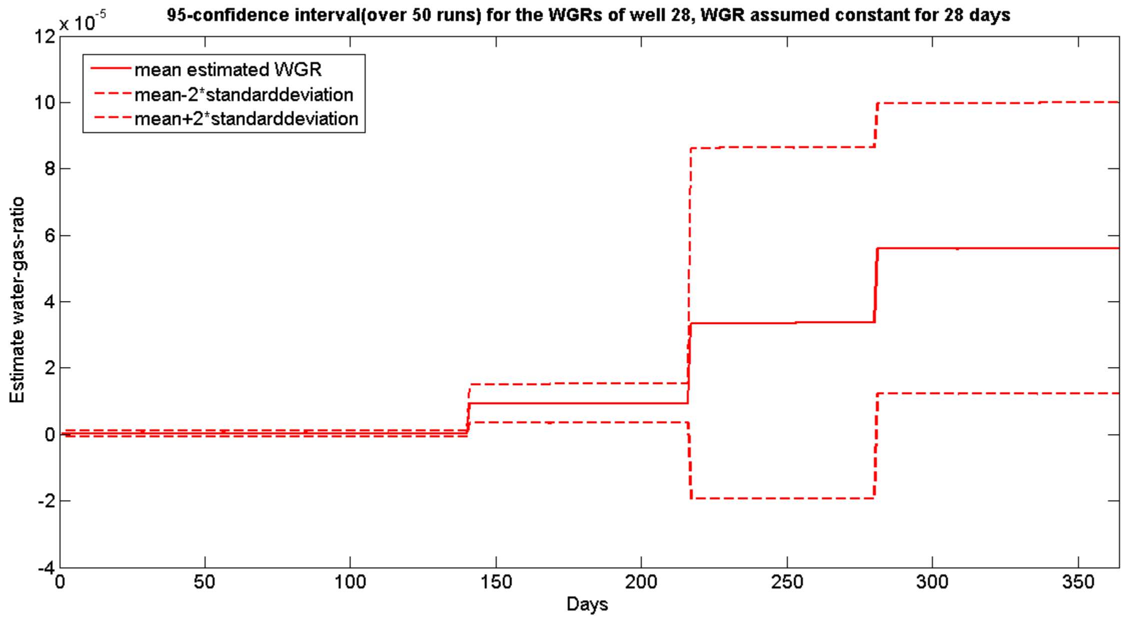

FIGURE 4.18. 95%-confidence intervals WGR (assumed constant for 28 days), well PS01

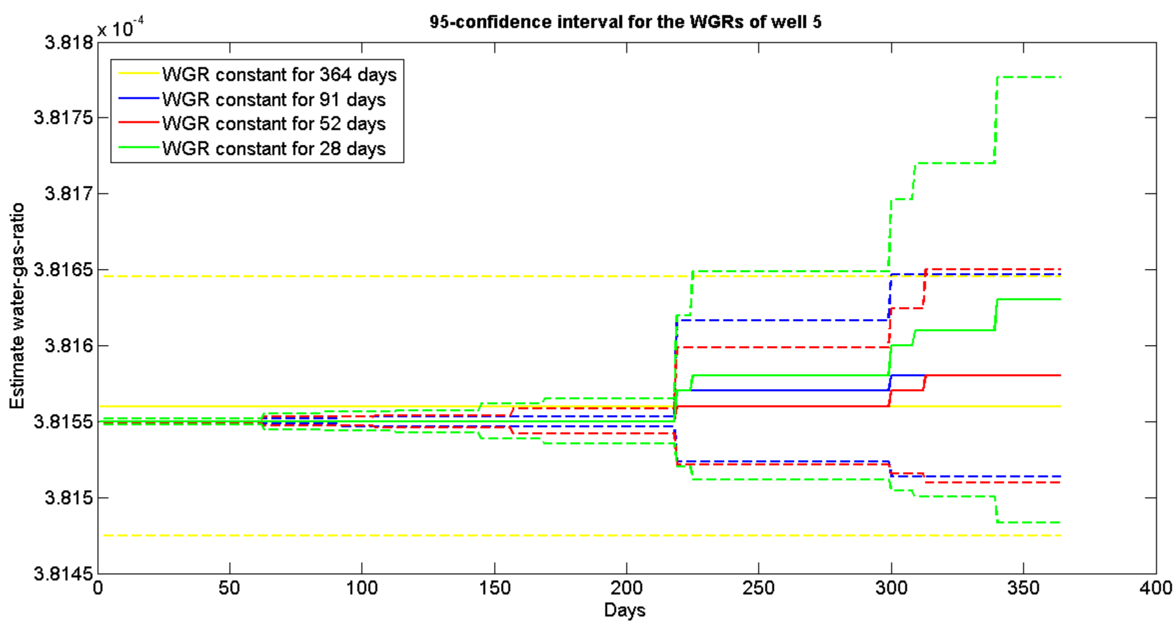

FIGURE 4.19. 95%-confidence intervals WGR (assumed constant for different periods), well PB11

For well PS01 the estimate of the WGR differs for the different periods, whereas for well PB11 the estimate of the WGR is the same and also the standard deviation is very small (the y-axis shows almost no change). For well PS01 the size is also uncertain, the 95%-intervals are quite wide. Note furthermore that the interval increases over the year. Because the algorithm takes the whole year into account, the periods over which the WGR is assumed constant 'communicate'; the other periods are taken into account as the WGR of one period is determined. As a consequence, in the beginning of the year less slack is possible than in the end of the year. This results in the larger intervals at the end of the year. The WGR of PB11 remains constant over the year, which is not very realistic. However, since the size is larger than the other wells one can imagine that the WGR increases slower than the wells of smaller order.

In Table 4.3 the errors can be found. These errors are the average over the 50 runs that were done.

WGR constant for	**Average 2-norm error**	**Average relative error**	**Run time(s)**
364 days	$2.0138 * 10^3$	61.01%	320.55
91 days	$1.5519 * 10^3$	44.02%	1978.47
52 days	$1.4898 * 10^3$	41.72%	4418.58
28 days	$1.4322 * 10^3$	39.66%	12938.79

Table 4.3. 2-norm and relative error averaged over all simulation runs

It can be seen that the errors are large. Furthermore, the (relative) error does hardly reduce if the period over which the WGR is assumed constant, decreases. The run time is large, as was expected from the long computation time of one run.

Chapter 5

Conclusions and recommendations

This chapter contains the conclusions of the report. After that recommendations for further research are done.

5.1 Conclusions

This report investigates the construction of a model to make precise, yet realistic estimates of the water production per well of wells offshore based on the gas and water production data. Precise estimates means that the error (difference between the measured and estimated production water) is as small as possible. An estimated WGR is defined as realistic if (1) WGRs which can only increase (exceptions allowed under specific circumstances) and (2) the size of WGRs is of the expected order based on the knowledge of the production programmer.
The water production is indicated by the WGR and provides valuable information about several aspects of the gas production process; for example the amount of gas left in the well and the amount of corrosion in the pipelines. Therefore, the water production per well is wanted as there are no facilities to measure the water rate for individual wells.

The problem is described mathematically by a minimization problem where the WGRs are estimated such that the difference between the measured and estimated water production is minimized. Constraints are added to ensure the requirements of realistic WGRs. The minimization problem is solved by a least-squares method. The algorithm to solve this large problem is the interior-point method. This method deals with the inequality constraint as a barrier method; the constraints are added to the objective function with the use of a barrier parameter and slack variables.

First the model was tested for a small-scale problem, the Sean area where five gas wells are present. In advance the production programmer knows that the WGRs should be of the same size. The model shows good results for the small-scale area: the errors are small and the estimates of the WGRs look similar to the current estimates but more realistic. The relative error is 5%, which confirms the good results. Two notes are made to these results; the model is very dependent on the initial guess for the WGRs and the number of iterations is larger than expected. However, it can be concluded that for a small-scale problem it is possible to estimate the WGRs precisely and realistic, based on the gas and water production data.

Secondly the model is applied to a large-scale problem, the Solepit area where 49 gas wells are present. The information from the production programmer, based on the well test, on the expected size of the WGRs is that there are four wells with a much larger WGR than the other wells. Because of this, the results are more difficult to compare to the current estimates. The model makes a relative error of $\approx 25\%$, which is rather large. This might be caused by the implementation of the well test. Another cause can be the time delay, which is very difficult to incorporate in the model. The long computational time of the model is not workable. For the large-scale problem it can be concluded that it is possible to make both realistic and precise estimates of the WGR, based on the gas and water production data.

The final model was also used to incorporate the errors of the measurements, which were neglected until now. Implementation is done by changing the solution method to weighted least-squares. The model is run 50 times with the measurements drawn from a Gaussian distribution. The confidence intervals and error made is large, which means that the estimates are not precise. Overall it is concluded that it is not possible to construct a model based on gas and water production data, for precise and realistic estimates of the WGR.

Suggestions to improve the results of the current model are listed below.

5.2 Recommendations

The work out carried in this report was done in a limited amount of time, such that not every option and detail could be considered. Therefore some recommendations are given below, which can be taken into account when this topic is studied more and in more detail.

5.2.1 Solution method

The least-squares method should be adapted to deal with the fluctuating behaviour of the gas and water production. There are a lot of outliers in the problem, whereas the ordinary LSM is not a robust method to outliers. An adaption of the LSM could be to change the solution method to weighted LSM (which was also used to incorporate the uncertainties). Lower weights could be given to the outliers. Note that there were a lot of outliers, so this adaption is cumbersome.

5.2.2 Use of the well test

The way in which the results of the well tests were used, was a first attempt. The well tests are very accurate and the information from it could be used in another way as well. Especially looking at the results of the simulation for the wells with a significant large WGR: the model did not contribute much here and there might be more possibilities here. For example as a check or update of a dynamic model, which is suggested below. An other small point of attention: the well test that is used was from this year, while the model was made for the data of the previous year. This meant that the results of the well test were adapted to being able to use them in the model. However, this adaption was a rough guess and could be improved. The time difference between the data and the well test will always exist. The gas and water data is available at the end of the year, where the well tests are performed throughout the year. Furthermore do the moments at which this happens, differ per platform.

5.2.3 Use of full dynamic model

From the conclusions it follows that the development of a purely data-driven model to find better estimates of the WGR, is very hard. Therefore it is suggested here to use a full dynamic model where physical aspects of the gas production process are included in addition to the data. To start with, the delay (coherent the sweep phenomenon) could be incorporated, which is a complicated process for which there are no fully developed models. The delay differs per pipeline (and thus per platform). If the delay is known, the gas data can be matched with the water production it caused. Another suggestion would be to implement that the WGR can decrease after a shutdown. During this study not enough information was known on how this could be implemented exactly, but investigating it is recommended. Lastly the dynamical model should implement more information from the well test. These measurements are very accurate and could be used to dynamically check or update the model.

References

Geology.com (2014). Shale, shale is the most abundant sedimentary rock and is in sedimentary basins worldwide. http://geology.com/rocks/shale.shtml. Accessed: 25-7-2014.

Heitman, I. (2014a). personal communication. position: ONEgas West Production Programmer.

Heitman, I. (2014b). personal communication. position: ONEgas West Production Programmer.

NAM (2014). Onze historie. http://www.nam.nl/nl/about-nam/our-history.html. Accessed: 14-2-2014.

Nocedal, J. and Wright, S. (2006). *Numerical Optimization*. Springer.

The Paleontological Research Institution (2014). Structural traps. http://www.priweb.org/ed/pgws/systems/traps/structural/structural.html. Accessed: 6-8-2014.

List of Figures

List of Tables

Appendix

A. Gas network offshore North Sea

This appendix contains pictures of the offshore gas network of the North Sea. There are close-ups given of the areas that are being used to construct the model in this report.

A.1 Complete gas network offshore North Sea

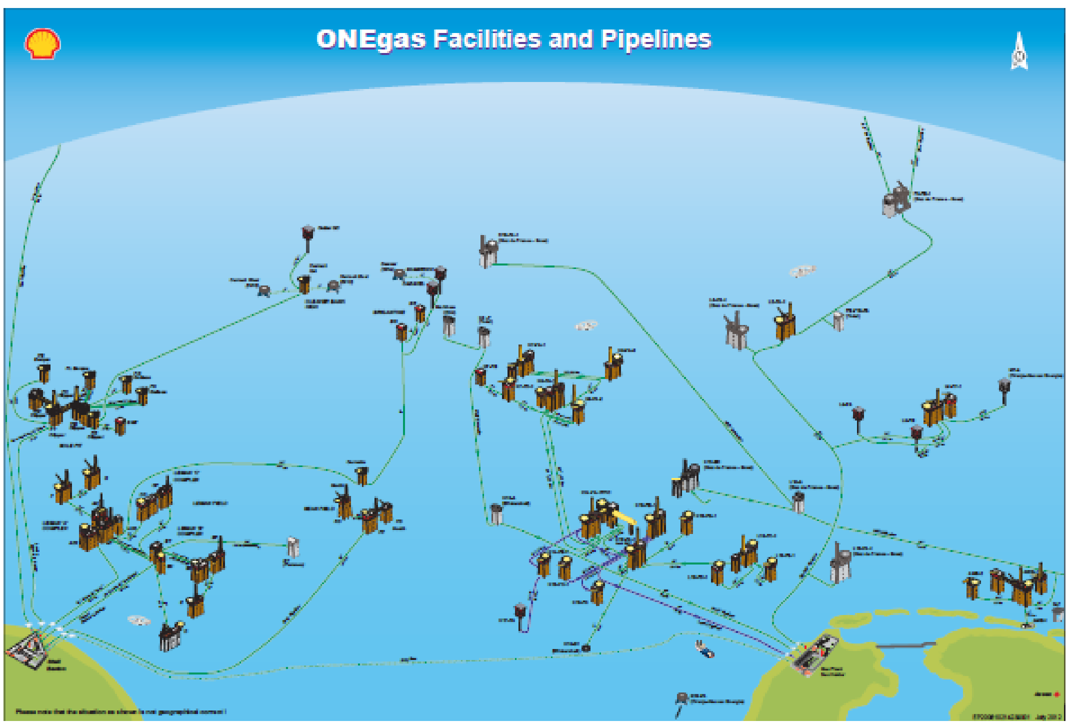

FIGURE A.1. Offshore gas network NAM North Sea (NAM, 2014)

Figure A.1 gives an overview of the whole gas network at the North Sea. The figure gives insight in the size of the network. And more relevant for the problem in this report, the distances between the different platforms.

A.2 Western part gas network NAM North Sea

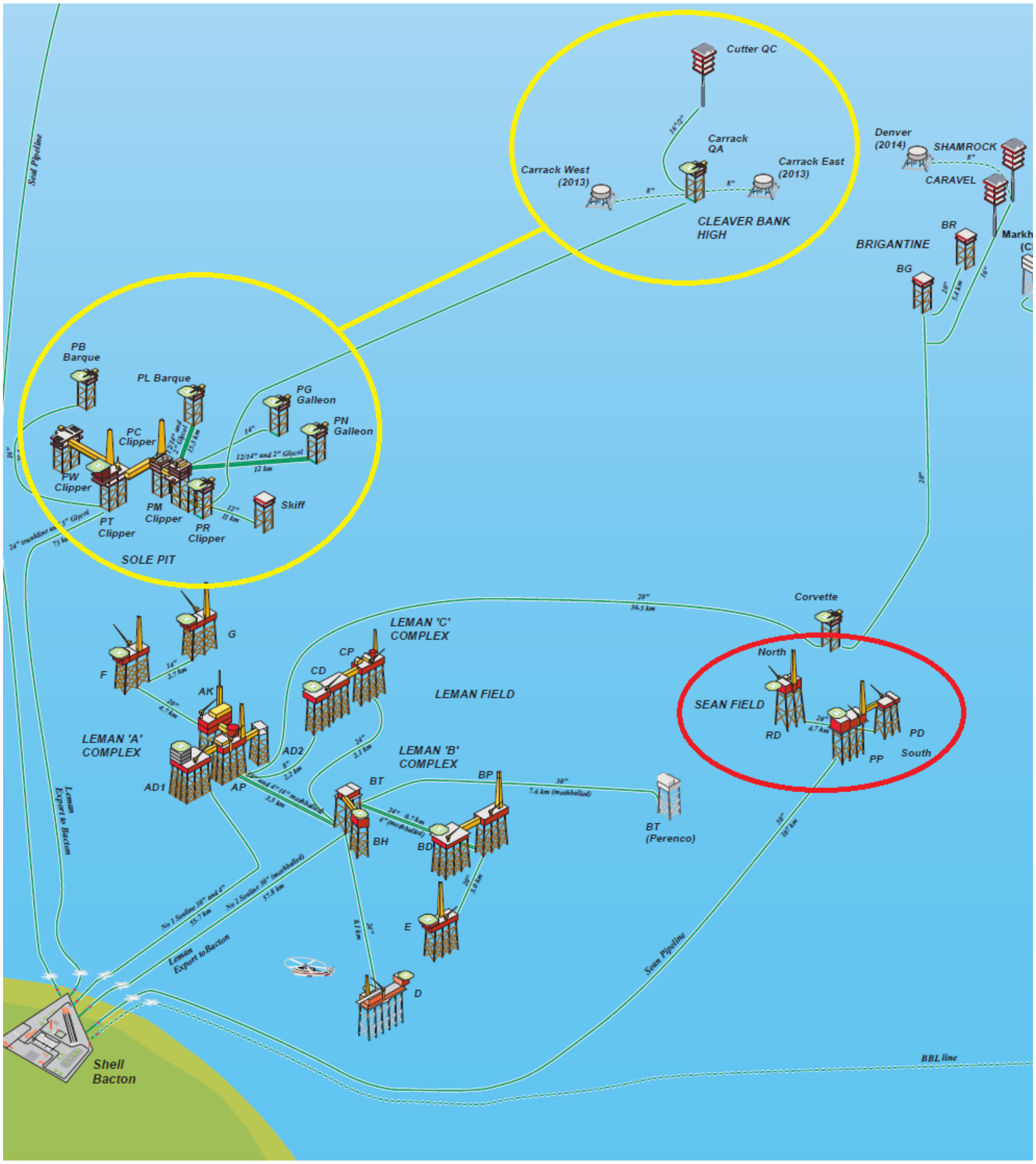

Figure A.2. Offshore gas network NAM North Sea Western part

Figure A.2 shows the offshore gas network in front of the coast of England. All gas produced from this network goes to the shore located at Bacton. The gas network that is first under consideration in the report is encircled by a red line, the Sean area. A closer view can be found in Figure A.3. The two parts that are encircled by the yellow line form the Solepit area. This can be viewed more closely in Figure A.4.

A.3 Sean and Solepit area

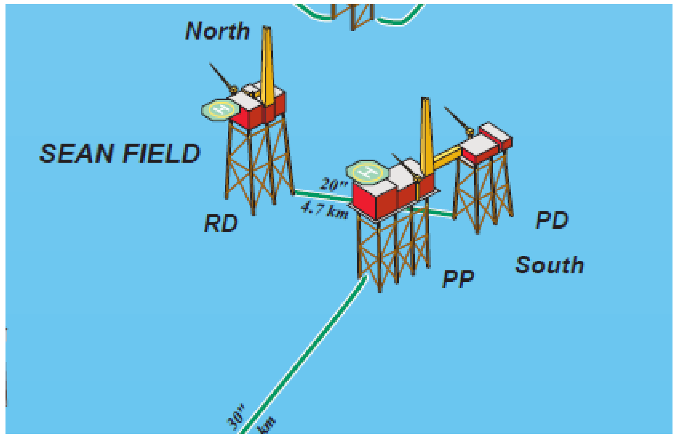

FIGURE A.3. Offshore gas network NAM Sean area

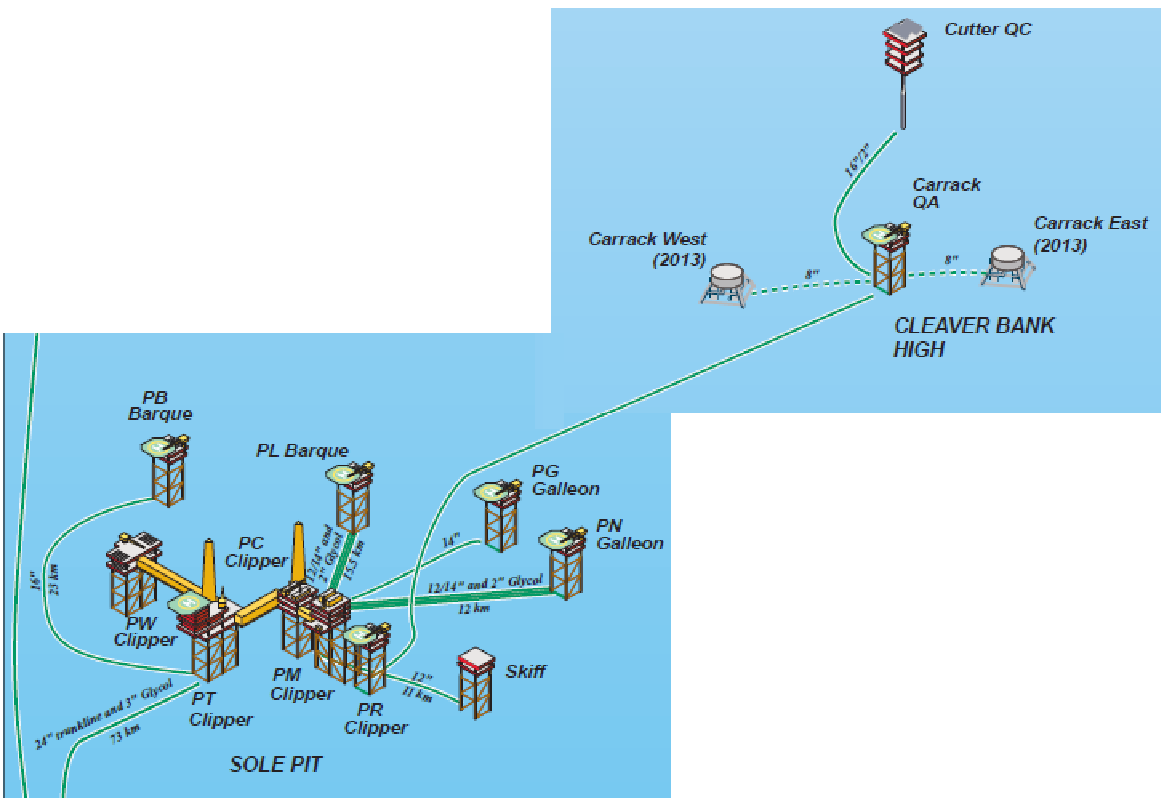

FIGURE A.4. Offshore gas network NAM Solepit area

As can be seen from the figures above the number of platforms and wells at the Sean area is small. Also, the distances are small(considering the velocity of the gas). The Solepit area on the other hand is much larger: there are a lot more platforms and wells. Also the pipelines are larger in both length and cross section.

A.4 Design parameters pipelines Solepit area

Platform	**Length pipe to Clipper**	**Diameter**	**Section**
	[m]	[inch]	[m^2]
PB	23000	16	0.1297
PG	-	14	0.0993
PL	15500	12	0.0730
PN	12000	12	0.0730
PS	11000	12	0.0730

TABLE A.1. Data about the pipelines between the platforms and the Clipper platform

B. Estimated WGRs Sean PD platform for all wells 2012

This appendix shows the WGRs of the wells platform PD at the Sean area over the year 2012 as estimated by the algorithm which is explained in chapter 3.

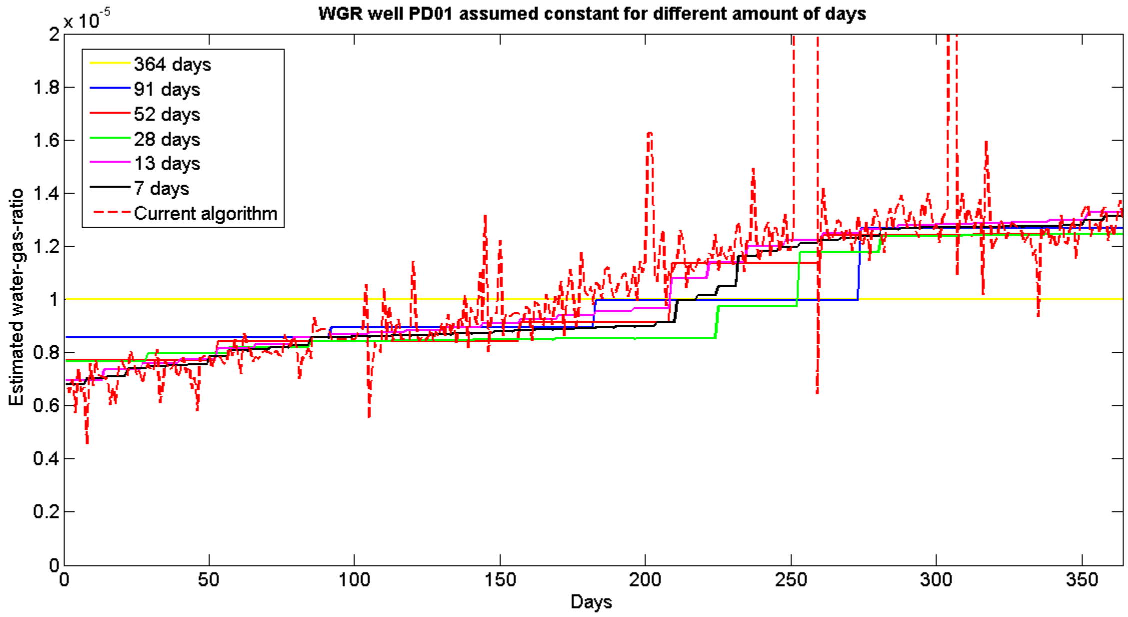

FIGURE B.1. WGR assumed constant over different periods and no decreasing allowed, well PD01

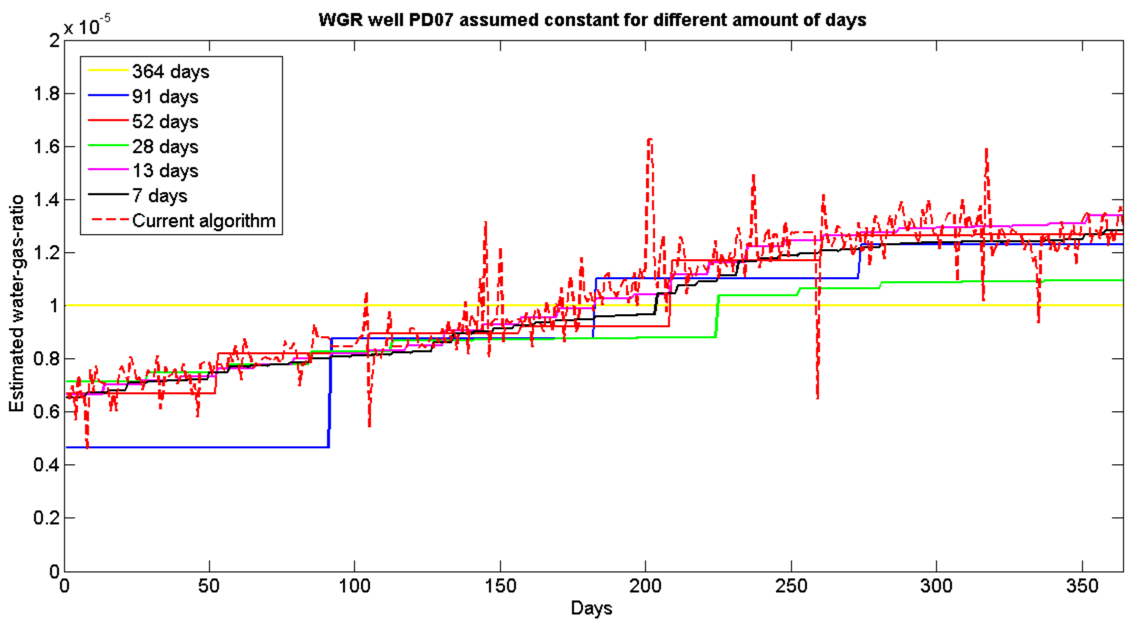

FIGURE B.2. WGR assumed constant over different periods and no decreasing allowed, well PD07

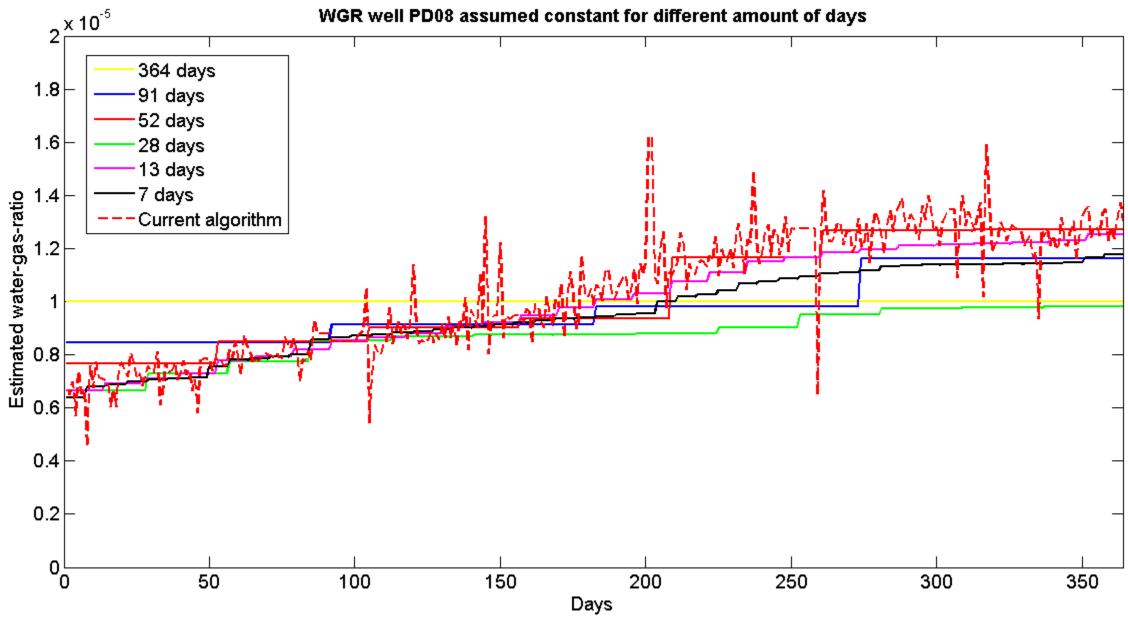

FIGURE B.3. WGR assumed constant over different periods and no decreasing allowed, well PD08

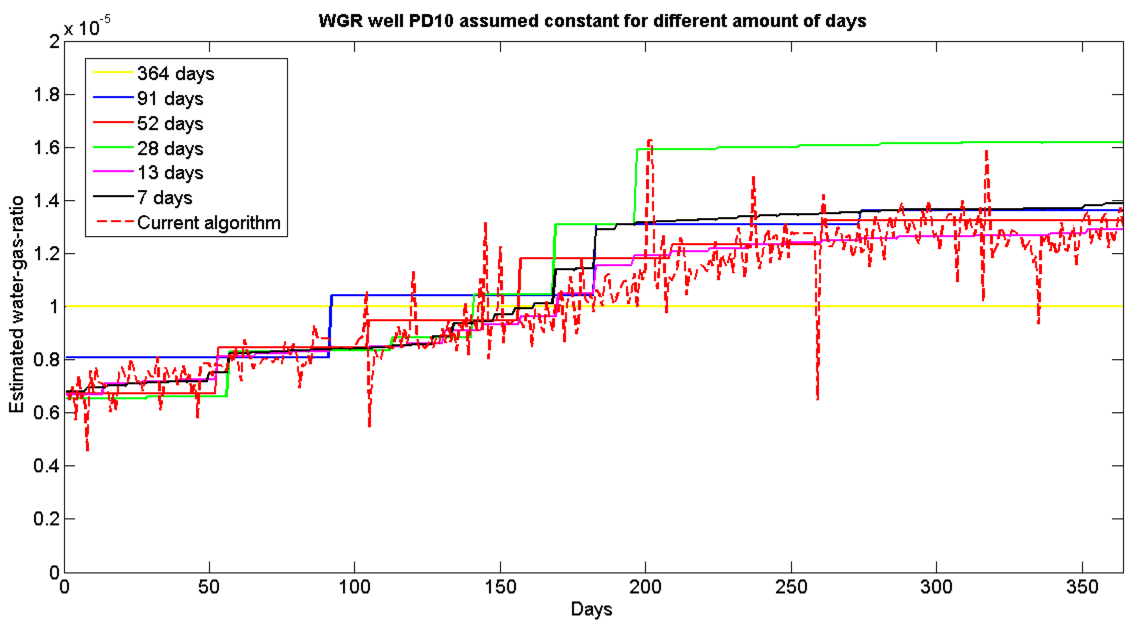

FIGURE B.4. WGR assumed constant over different periods and no decreasing allowed, well PD10

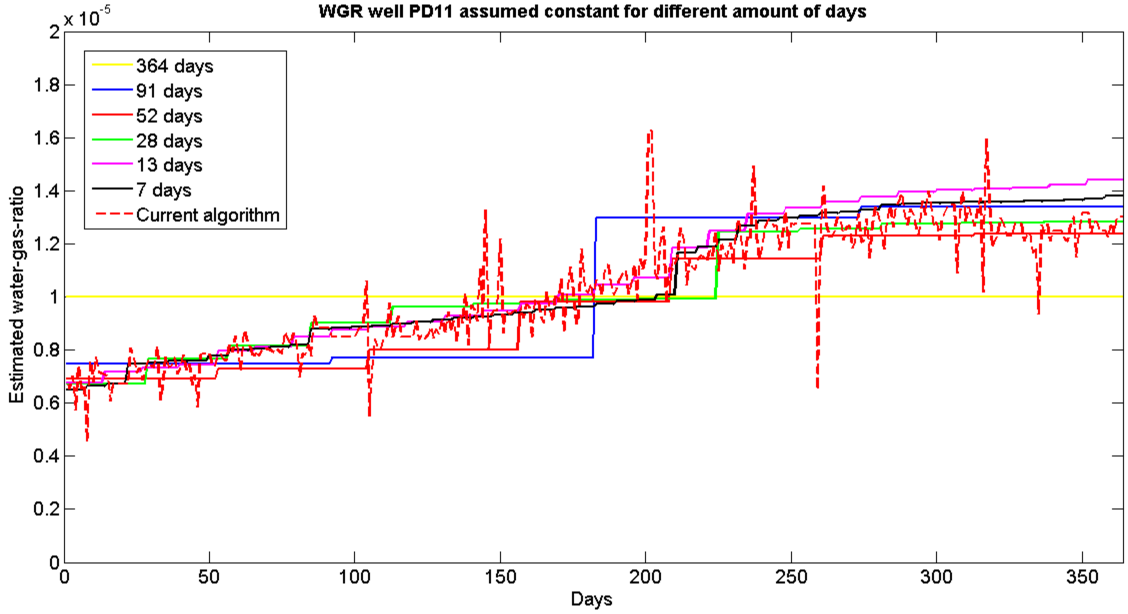

FIGURE B.5. WGR assumed constant over different periods and no decreasing allowed, well PD11

As can be seen from the figures, the WGRs from the wells show similar behaviour and are of the same order. The estimate of the WGR when assumed constant for a week and two weeks in Figure B.5 deviates more from the current estimates compared to the other wells. This can be explained by the gas production data of this well. During the end of the year, this well switches often between producing gas and not producing gas and the gas production is of the same size as the other wells. This results in larger WGRs because days on which there is no gas production needs to be compensated by the days on which there is a gas production.

C. WGRs Solepit area 2013

This appendix gives the WGRs of the current estimation process for all wells(except for the wells at platform PL which are already given in section 4.3) of the greater Solepit area in the year 2013.

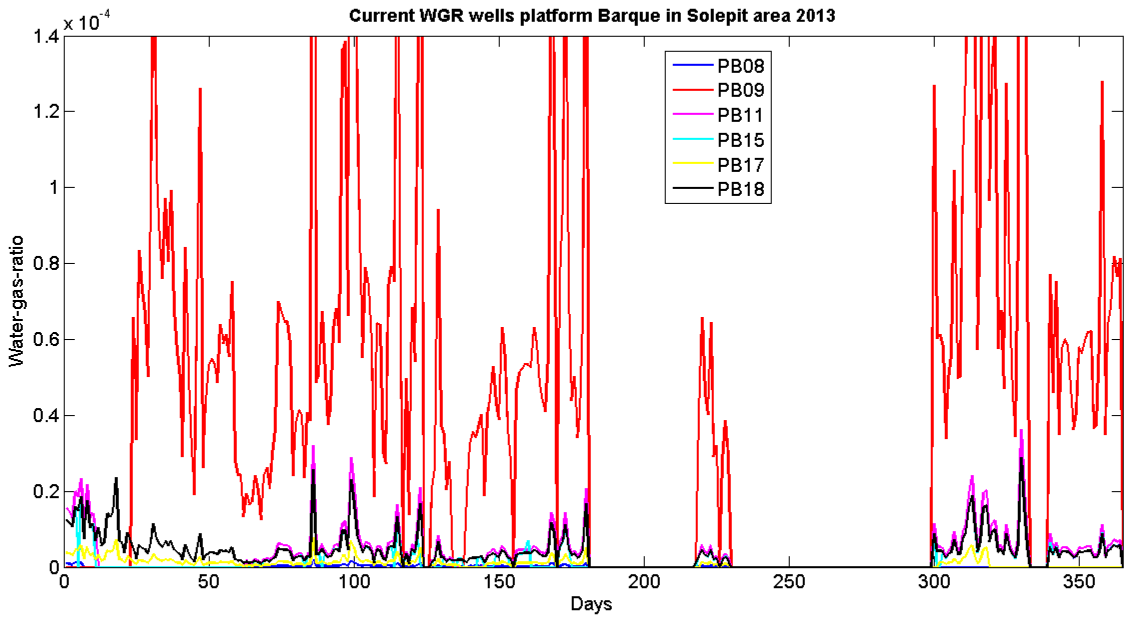

FIGURE C.1. Current WGR estimates PB platform, Solepit area 2013

Figure C.1 shows the WGRs of platform PB calculated by the current algorithm. Notice that the platform has nine wells in total, whereas the figure shows the WGRs of only six wells. Well PB04, PB10 and PB16 did not produce gas in 2013 and therefore their WGRs are not considered.

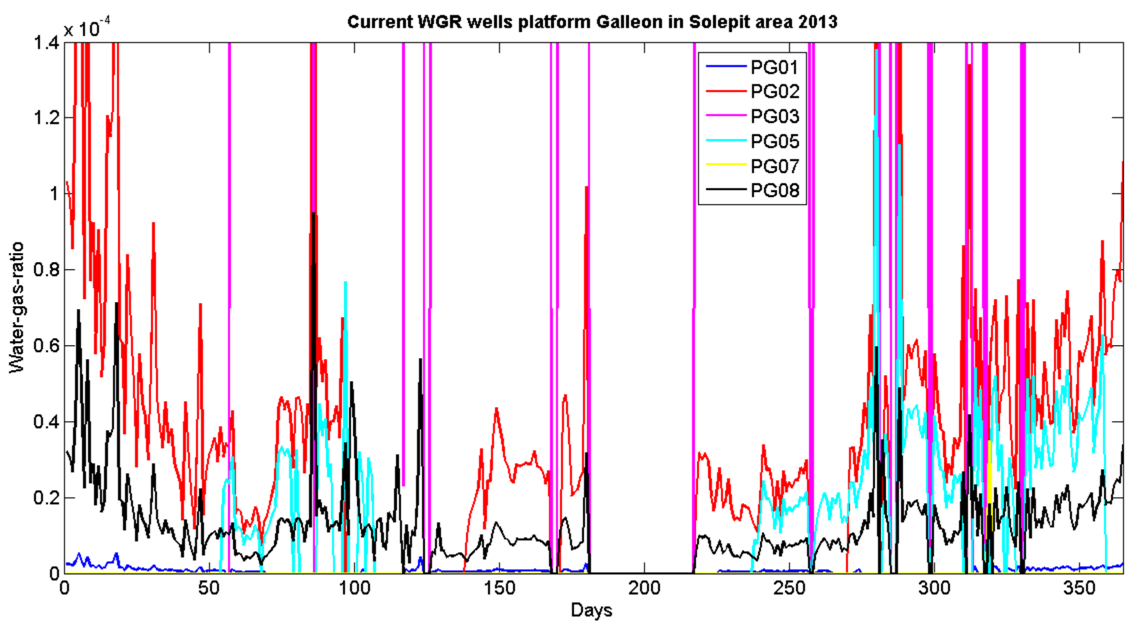

FIGURE C.2. Current WGR estimates PG platform, Solepit area 2013

In Figure C.2 the WGR of well PG04 was excluded because it was not producing gas in 2013.

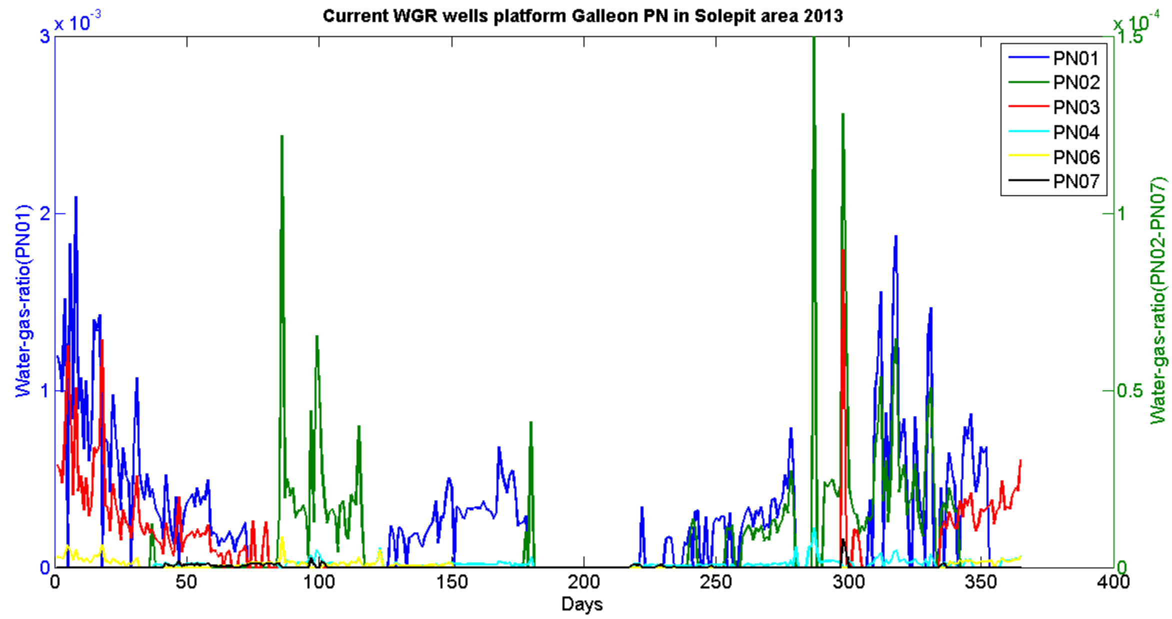

FIGURE C.3. Current WGR estimates PN platform, Solepit area 2013

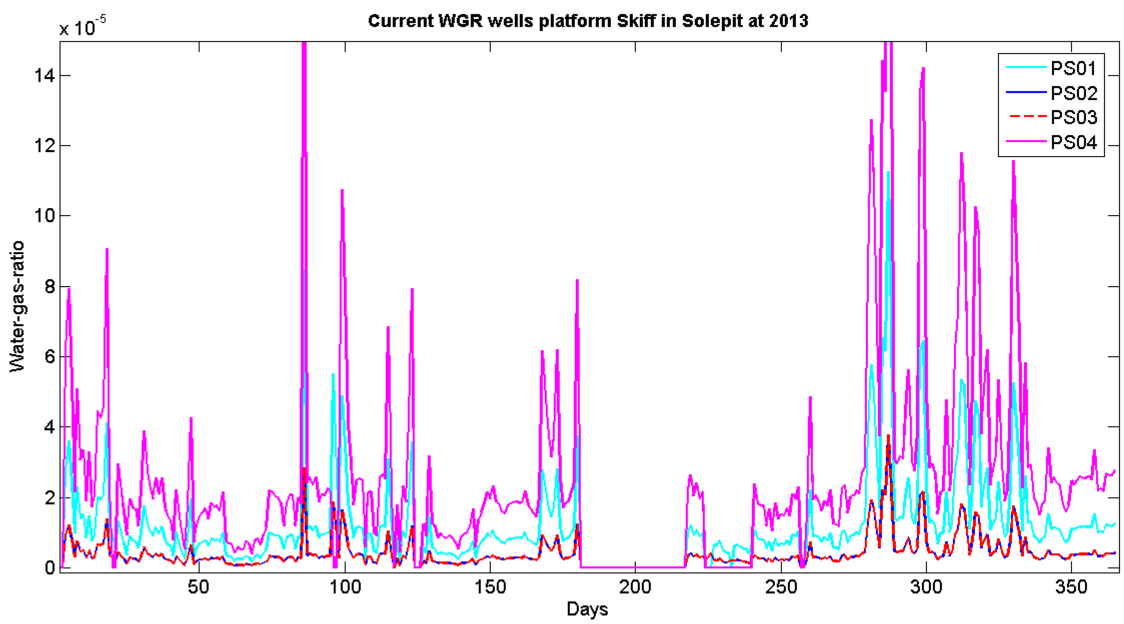

FIGURE C.4. Current WGR estimates PS platform, Solepit area 2013

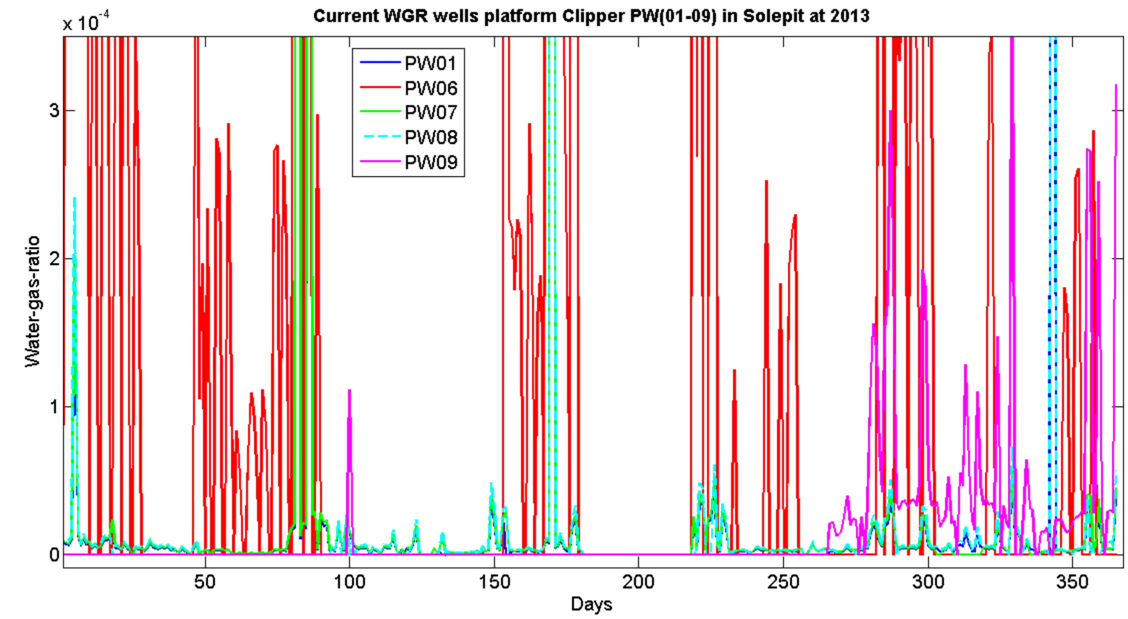

FIGURE C.5. Current WGR estimates PW platform(wells 01-09), Solepit area 2013

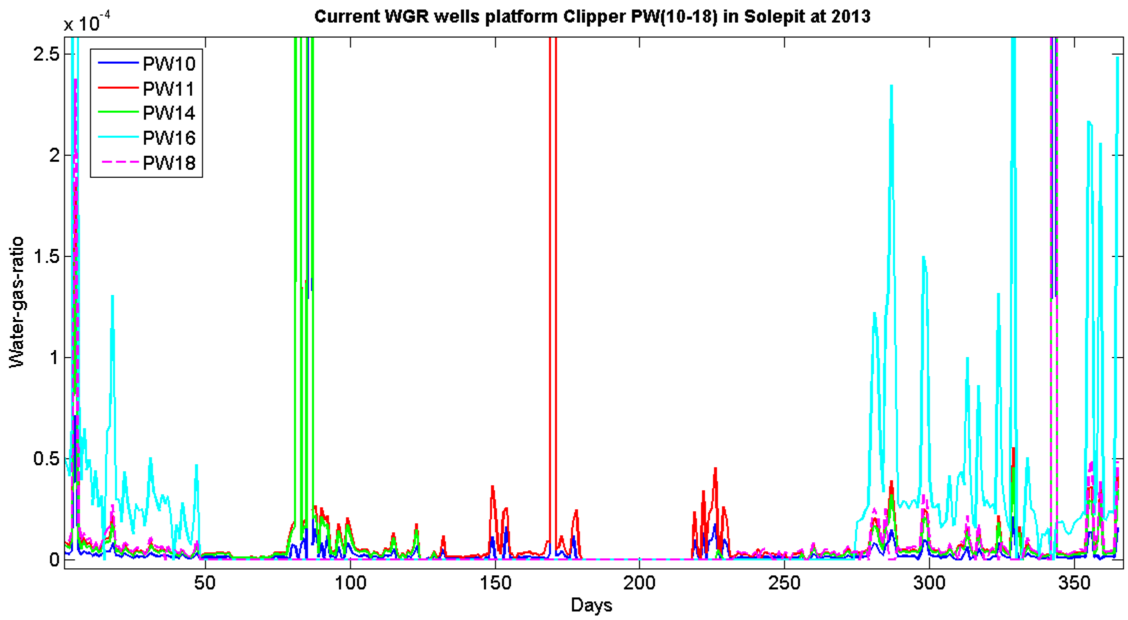

FIGURE C.6. Current WGR estimates PW platform(wells 10-18), Solepit area 2013

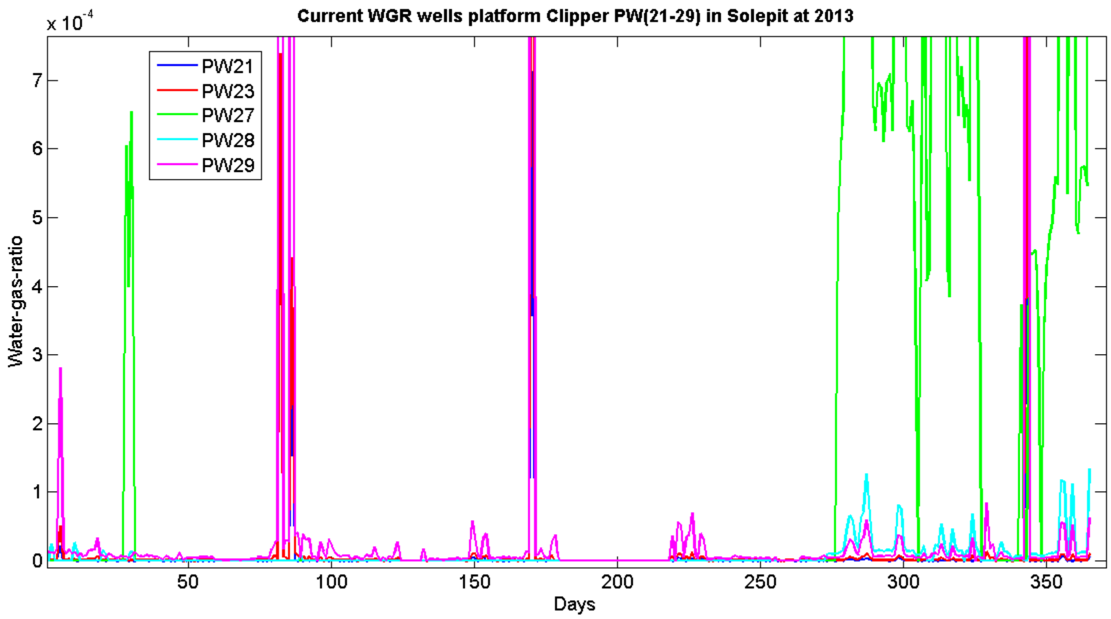

FIGURE C.7. Current WGR estimates PW platform(wells 21-29), Solepit area 2013

From the figures some conclusions can be drawn from the current estimates of the WGR:

- The WGRs fluctuate a lot and quickly. As shown in the main text(setion 4.3) this is not caused by the behaviour of the gas production; most probably they are modeling errors.
- The WGRs are of the same order, with a few exceptions.

D. Well test Solepit area 2014

This appendix contains the results of the well tests performed at different moments for each well, but all of them in 2014.

D.1 Results well test Solepit

A well test contains accurate information on various parameters of the well. The most important parameters of the well test are:

- The theoretical capacity of the well: the rate of gas the well can produce at the most.
- The availability of the well: how much of the capacity can actually be used.
- The actual capacity of the well: the rate of gas the well can produce actually. Notice that it is not possible for all wells to produce at this actual capacity, because the capacity of the pipe from the satellite platform to the main platform Clipper is usually less than the sum of the wells at the satellite platform together.
- The water-gas-ratio: the amount of barrels water(bbl) per million standard cubic feet(MMscf, common unit for a volume of gas) gas that is produced.
- The condensate-gas-ratio: the amount of barrels condensate per million standard cubic feet gas that is produced.

The results of the most recent well test can found in the Table D.1-D.6. If the well and its data is coloured red, it means that this well was not producing/operating.

Well ↓	**Capacity [TJ]**	**Availability**	**Act.Cap. [TJ]**	**WGR [bbl/MMscf]**	**CGR [bbl/MMscf]**
PB16	23	100%	23	1.5	0.5
PB18	13	100%	13	18	0.5
PB11	3	100%	3	180	0.5
PB17	4	100%	4	2	0.5
PB09	4	100%	4	3.5	0.5
PB15	3	100%	3	155	0.5
PB08	3	100%	3	1	0.5
PB10	2.5	100%	2.5	-	-
PB04	5	0%	0	55	0.5

Table D.1. Most important information well test platform PB, 7-2-2014

Note that well PB04 is not producing gas(which corrensponds to well 1 in Figure 4.2. From the data of 2013 it was also seen that PB10 did not produce natural gas. As noticed in the main text of the report, here we see that the production rate and the water production are not correlated. Although PB16 has the largest production capacity, it has a very small water-gas-ratio. The opposite holds for PB11, which has a small production rate but a huge water-gas-ratio.

Well ↓	Capacity [TJ]	Availability	Act.Cap. [TJ]	WGR [bbl/MMscf]	CGR [bbl/MMscf]
PG01	10	100%	10	1.5	0.8
PG08	7	100%	7	5	0.8
PG03	4	100%	4	6.5	0.8
PG05	4	90%	3.6	> 33	0.8
PG02	4	100%	4	0.5	0.8
PG07	23	0%	0	10	0.8
PG04	1	0%	0	> 39	0.8

TABLE D.2. Most important information well test platform PG,7-2-2014

Well PG04 and PG07 can not produce gas, as was also seen in Figure 4.2.

Well ↓	Capacity [TJ]	Availability	Act.Cap. [TJ]	WGR [bbl/MMscf]	CGR [bbl/MMscf]
PL03	12	100%	12	0.5	0.5
PL01	5	100%	5	0.9	0.5
PL07	7	100%	7	0.6	0.5
PL02	5	100%	5	1.5	0.5
PL05	5	100%	5	0.7	0.5

TABLE D.3. Most important information well test platform PL, 26-3-2014

Well ↓	Capacity [TJ]	Availability	Act.Cap. [TJ]	WGR [bbl/TJ]	CGR [bbl/TJ]
PN02	11	100%	0	30	0.8
PN04	18	100%	0	1	0.8
PN03	9	Not available	0	2.5	0.8
PN06	18	30%	0	0.2	0.8
PN01	1	Not available	0	163	0.8
PN07	2	Not available	0	5.5	0.8

TABLE D.4. Most important information well test platform PN, 20-6-2014

From Table D.4 it looks as if none of the wells are producing gas. This seems like a measuring error, because from the data over 2013 all of the wells were producing gas. Note that the water/condensate-gas-ratio is given in a different unit. Below the conversion between TJ and MMscf will be given:

$$\begin{aligned}
1TJ &= 1*10^6 MJ \\
&= \frac{1*10^6}{HV} m^3 \\
&= \frac{1*10^6}{37} m^3 \\
&= \frac{1*10^6}{37} * 35.52 scf \\
&\approx 1*10^6 scf \\
&= 1MMscf
\end{aligned}$$

where HV is the heating value of natural gas, given in MJ/m^3.

Thus, the assumption is made that 1 TJ is equal to 1 MMscf.

Well ↓	**Capacity [TJ]**	**Availability**	**Act.Cap. [TJ]**	**WGR [bbl/MMscf]**	**CGR [bbl/MMscf]**
PS04	2	100%	2	6.6	-
PS03	7	100%	7	0.8	-
PS01	5	100%	5	3	-
PS02	8	100%	8	0.001	-

Table D.5. Most important information well test platform PS, 3-10-2013

Well ↓	**Capacity [TJ]**	**Availability**	**Act.Cap. [TJ]**	**WGR [bbl/MMscf]**	**CGR [bbl/MMscf]**
PW11	3	100%	3	1	-
PW24	4.5	100%	4.5	1	-
PW10	3	80%	2.4	1	-
PW29	3.5	100%	3.5	2	-
PW01	2.3	100%	2.3	2	-
PW14	2.5	100%	2.5	1	-
PW07	2	60%	1.2	1	-
PW16	3.6	100%	3.6	9	-
PW08	0.7	60%	0.42	1	-
PW27	1.6	100%	1.6	220	-
PW21	0.7	67%	0.47	1	-
PW28	1.1	100%	1.1	25	-
PW09	0.5	50%	0.25	5.9	-
PW18	0.4	75%	0.3	1	-
PW23	3.6	75%	2.7	1	-
PW06	0.7	8%	0.06	2	-
PW17	0.62	20%	0.12	1	-
PW12	4	0%	0	2.59	-

Table D.6. Most important information well test platform PW, 7-2-2014

Well PW12 can not produce gas, as was also seen in Figure 4.2.

It can be concluded from Table D.1-D.6 that the WGRs differ a lot. The next part of this chapter discusses the size of the WGRs and categorizes them based on their size.

D.2 Overview significant WGRs

Table D.7 contains the WGRs of all wells. The colors indicate the following:

- Red: this well did not produce gas in 2013.
- Green: this well has a very large WGR.
- Yellow: this well has a large WGR.
- Blue: this well has a larger WGR than the majority of the wells.

The WGRs from the well test are measured in the unit bbl/MMscf. This will be converged to $m^3(water)/m^3(gas)$ since that is the unit the WGRs are estimated by the model. This conversion is given below:

$$
\begin{aligned}
1\frac{bbl}{MMscf} &= 120\frac{L}{MMscf} \\
&= 0.12\frac{m^3}{10^6 scf} \\
&= 0.12\frac{m^3}{10^6 * 0.0283...m^3} \\
&= 4.240 * 10^{-6}\frac{m^3(water)}{m^3(gas)}
\end{aligned}
$$

Note that the WGRs in Table D.7 are the results from the well test in 2014, which were thus halved first to represent the WGRs from the year 2013.

Well ↓	**WGR** [bbl/MMscf]	**WGR** [m^3/m^3]	Well ↓	**WGR** [bbl/MMscf]	**WGR** [m^3/m^3]
PB04	55	-	PN01	163	$6.9102 * 10^{-4}$
PB08	1	$4.2394 * 10^{-6}$	PN02	30	$1.2718 * 10^{-4}$
PB09	3.5	$1.4838 * 10^{-5}$	PN03	2.5	$1.0599 * 10^{-5}$
PB10	2.5	-	PN04	1	$4.2394 * 10^{-6}$
PB11	180	$7.6309 * 10^{-4}$	PN06	0.2	$8.4788 * 10^{-7}$
PB15	155	$6.5711 * 10^{-4}$	PN07	5.5	$2.3317 * 10^{-5}$
PB16	1.5	$6.3591 * 10^{-6}$	PW01	2	$8.4788 * 10^{-6}$
PB17	2	$8.4788 * 10^{-6}$	PW06	2	$8.4788 * 10^{-6}$
PB18	18	$7.6309 * 10^{-5}$	PW07	1	$4.2394 * 10^{-6}$
PG01	1.5	$6.3591 * 10^{-6}$	PW08	1	$4.2394 * 10^{-6}$
PG02	0.5	$2.1197 * 10^{-6}$	PW09	5.9	$2.5012 * 10^{-5}$
PG03	6.5	$2.7556 * 10^{-5}$	PW10	1	$4.2394 * 10^{-6}$
PG04	> 39	-	PW11	1	$4.2394 * 10^{-6}$
PG05	≈ 40	$1.6958 * 10^{-4}$	PW12	2.59	-
PG07	10	-	PW14	1	$4.2394 * 10^{-6}$
PG08	5	$2.1197 * 10^{-5}$	PW16	9	$3.8155 * 10^{-5}$
PL01	0.9	$3.8155 * 10^{-6}$	PW17	1	$4.2394 * 10^{-6}$
PL02	1.5	$6.3591 * 10^{-6}$	PW18	1	$4.2394 * 10^{-6}$
PL03	0.5	$2.1197 * 10^{-6}$	PW21	1	$4.2394 * 10^{-6}$
PL05	0.7	$2.9676 * 10^{-6}$	PW23	1	$4.2394 * 10^{-6}$
PL07	0.6	$2.5436 * 10^{-6}$	PW24	1	$4.2394 * 10^{-6}$
PS01	3	$1.2718 * 10^{-5}$	PW27	220	$9.3267 * 10^{-4}$
PS02	0.001	$4.2394 * 10^{-9}$	PW28	25	$1.0599 * 10^{-4}$
PS03	0.8	$3.3915 * 10^{-6}$	PW29	2	$8.4788 * 10^{-6}$
PS04	6.6	$2.7980 * 10^{-5}$			

TABLE D.7. WGRs well test Solepit area, 2014

E. Results Solepit-algorithm more significant WGRs in well test

E.1 Solepit-algorithm six wells having a lower bound based on the well test

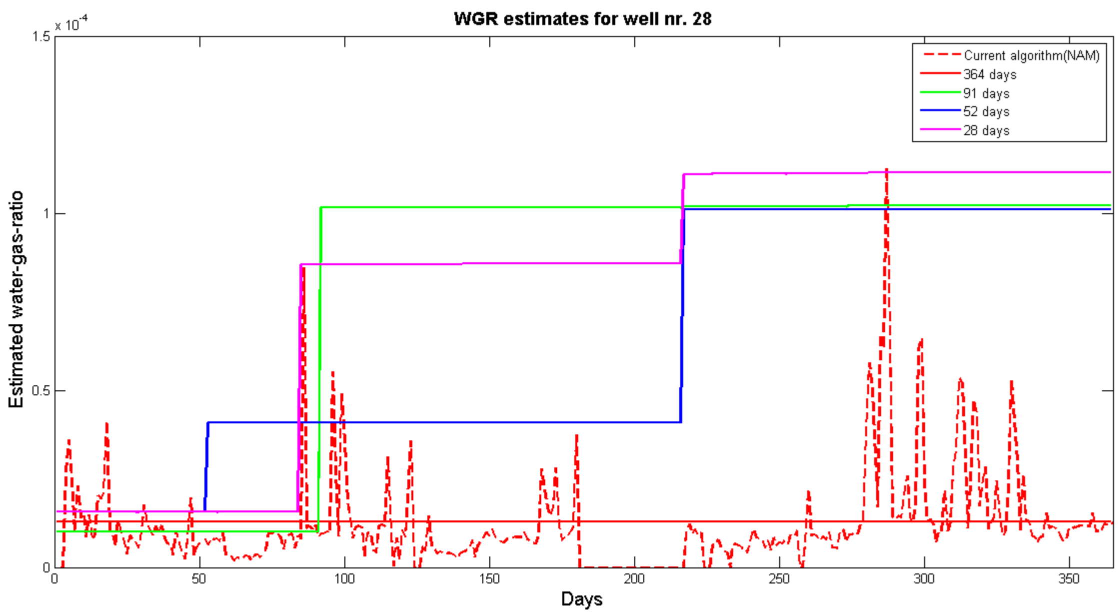

FIGURE E.1. WGR assumed constant over different periods, well PS01 Solepit 2013 (six wells having a lower bound based on well test)

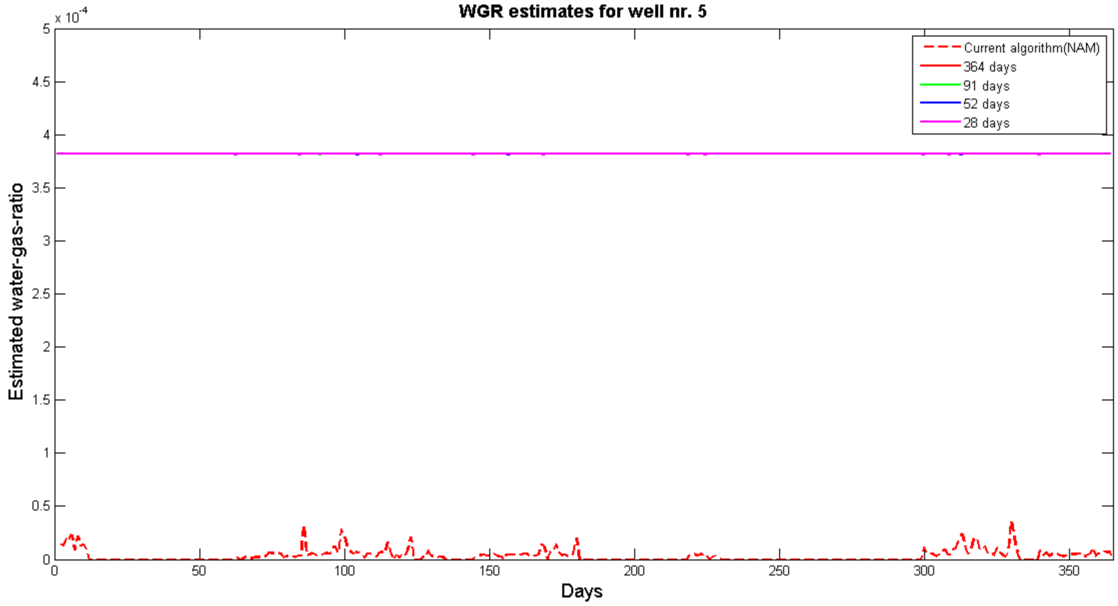

FIGURE E.2. WGR assumed constant over different periods, well PB11 Solepit 2013 (six wells having a lower bound based on well test)

Time constant	Average 2-norm error	Average relative error
364 days	947.7441	0.2826
91 days	843.5314	0.2457
52 days	857.5822	0.2511
28 days	838.8891	0.2423

TABLE E.1. 2-norm and relative error Solepit algorithm (six wells having a lower bound based on well test)

E.2 Solepit-algorithm eight wells having a lower bound based on the well test

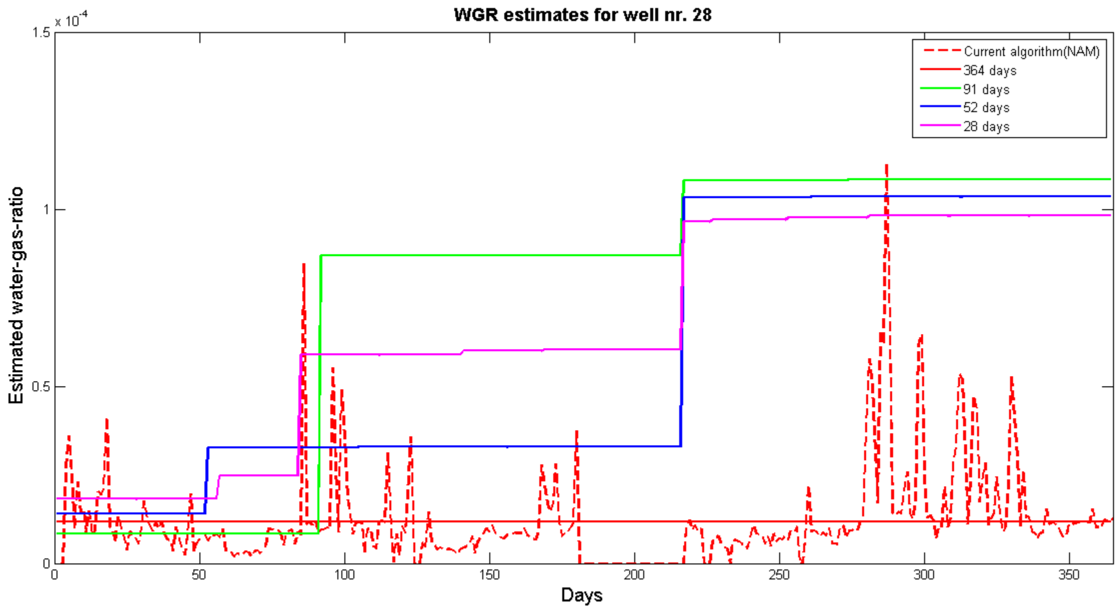

FIGURE E.3. WGR assumed constant over different periods, well PS01 Solepit 2013 (eight wells having a lower bound based on well test)

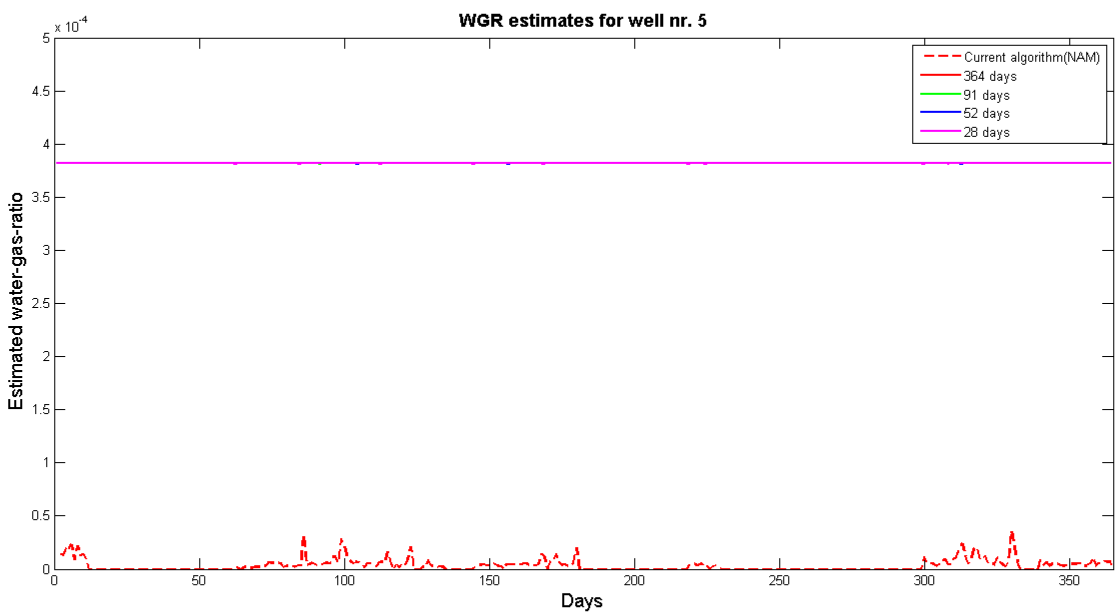

FIGURE E.4. WGR assumed constant over different periods, well PB11 Solepit 2013 (eight wells having a lower bound based on well test)

Time constant	Average 2-norm error	Average relative error
364 days	963.2748	0.2875
91 days	861.2979	0.2499
52 days	877.7867	0.2580
28 days	883.7163	0.2572

Table E.2. 2-norm and relative error Solepit algorithm (eight wells having a lower bound based on well test)